CAPITAL UNIVERSITY OF SCIENCE AND TECHNOLOGY, ISLAMABAD

Protective Effects of Mecobalamin Against Cisplatin-Induced Nephrotoxicity in Mice

by

Sania Khan

A thesis submitted in partial fulfillment for the degree of Master of Philosophy

in the

Department of Pharmacy
Faculty of Pharmacy

2025

Dedicated to my Parents your unwavering love, support and prayers have been my guiding light throughout this journey. This work is a small reflection of the strength and inspiration you have always been in my life. I dedicate this thesis to you with all my heart.

Also I dedicate this to my beloved Ishtiaq Mamu (Late), though you are no longer with us in this world, your love, wisdom and quiet strength continue to live in my heart. Your memory has been a source of comfort and motivation throughout this journey. I wish you were here to share this moment, but I know you're watching over me with pride. This thesis is dedicated to you my dear Ishtiaq Mamu (Late) with love, longing and endless gratitude.

CERTIFICATE OF APPROVAL

Protective Effects of Mecobalamin Against Cisplatin-Induced Nephrotoxicity in Mice

by

Sania Khan

(MPH233004)

THESIS EXAMINING COMMITTEE

S. No.	Examiner	Name	Organization
(a)	External Examiner	Dr. Maqsood ur Rehman	UoM, KPK
(b)	Internal Examiner	Dr. Siraj Khan	CUST, Islamabad
(c)	Supervisor	Dr. Fazlullah Khan	CUST, Islamabad

Fazlullah Khan
Thesis Supervisor
September, 2025

Dr. Fazlullah Khan
Head
Dept. of Pharmacology
September, 2025

Dr. Muzzaffar Abbas
Dean
Faculty of Pharmacy
September, 2025

Author's Declaration

I, **Sania Khan** hereby state that my MPhil thesis titled "**Protective Effects of Mecobalamin Against Cisplatin-Induced Nephrotoxicity in Mice**" is my own work and has not been submitted previously by me for taking any degree from Capital University of Science and Technology, Islamabad or anywhere else in the country/abroad.

At any time if my statement is found to be incorrect even after my graduation, the University has the right to withdraw my MPhil Degree.

(Sania Khan)

Registration No: MPH233004

Plagiarism Undertaking

I solemnly declare that research work presented in this thesis titled "**Protective Effects of Mecobalamin Against Cisplatin-Induced Nephrotoxicity in Mice**" is solely my research work with no significant contribution from any other person. Small contribution/help wherever taken has been duly acknowledged and that complete thesis has been written by me.

I understand the zero tolerance policy of the HEC and Capital University of Science and Technology towards plagiarism. Therefore, I as an author of the above titled thesis declare that no portion of my thesis has been plagiarized and any material used as reference is properly referred/cited.

I undertake that if I am found guilty of any formal plagiarism in the above titled thesis even after award of MPhil Degree, the University reserves the right to withdraw/revoke my MPhil degree and that HEC and the University have the right to publish my name on the HEC/University website on which names of students are placed who submitted plagiarized work.

(Sania Khan)

Registration No: MPH233004

Acknowledgement

In the name of Allah, the Most Gracious, the Most Merciful. All praise is due to Allah, the Lord of the worlds. With a heart full of humility and gratitude, I begin by offering my eternal thanks to **Almighty Allah (SWT)**, the ultimate source of knowledge, patience, and strength. Through His infinite mercy and boundless grace, I found the courage to persist, the wisdom to learn, and the serenity to overcome every challenge along this academic journey. I send peace and blessings upon our beloved **Prophet Muhammad (PBUH)**, whose life remains a radiant beacon of faith, whose teachings of compassion, knowledge, and perseverance continue to illuminate the path for seekers of truth and knowledge around the world.

I am profoundly grateful to my distinguished supervisor, **Dr. Fazlullah Khan Associate Professor (Head of department Pharmacology, Faculty of Pharmacy, Capital University of Science and Technology, Islamabad)**. His insightful mentorship, inspiring leadership, and constant encouragement elevated the quality of my work and nurtured my growth as a researcher. His passion for science, clarity of thought, and compassionate guidance has left a lasting mark on my academic life.

To the **Capital University of Science and Technology, Islamabad**, I am thankful for providing a platform where learning and discovery could flourish.I extend heartfelt thanks to **Prof Dr. Muzzffar Abbas (Dean Faculty of Pharmacy, Capital university of science and Technology , Islamabad)**, whose support, both academic and personal, helped shape this endeavour and made the environment at CUST rich with knowledge

I would like to express my deepest gratitude to my **Parents** for their unconditional love, support and sacrifices throughout my academic journey. Their constant encouragement, patience and unwavering belief in my abilities have been the foundation of my strength.

From the very beginning they instilled in me the values of hardwork, preservence and integrity which have guided me not only in my studies but also in life. Their prayers, moral support and motivation have been instrumental in helping me reach this milestone.

This thesis is reflection of their dedication and a small token of appreciation for everything they have done for me.

I would like to express my deepest gratitude to my dear Husband for his endless support, patience and encouragement throughout the course to my Mphil studies.His unwavering belief in me has been a constant source of strength and motivation.

Thank you for your understanding during long hours of research and writing and for being my pillar of support through every challenge. Your love, sacrifices, and silent strength have played a significant role in helping me reach this important milestone.

This achievement is as much yours as it is mine.

I would like to extend my heartfelt gratitude to my brothers & family for their unwavering support, patience and encouragement throughout my MPhil journey.

I would also like to sincerely thank my lab technicians, class fellows and colleagues for their valuable support, insightful discussions. I appreciate the positive and stimulating environment they helped create, which has been vital to my growth as a researcher. I am truly blessed and thankful to have had them by my side.

(Sania Khan)

Abstract

Cisplatin induced nephrotoxicity is a significant clinical and public health concern due to oxidative stress, diseases caused by immune dysfunction, and persistent chronic inflammation that sustain kidney injury. Glutathione , NADPH is an important mediator of kidney oxidative stress, inflammation through the formation of pro-inflammatory prostaglandins and activation of TNFα. Mecobalamin offers a supportive therapeutic modality that has no gastrointestinal side-effects. In this study, we examined the nephroprotective effects of mecobalamin compared to silymarin, as a supportive treatment in an animal model of cisplatin induced nephrotoxicity. Nephrotoxicity was induced with cisplatin (10 mg/kg, i.p.) single dose and observed for 10 days. The treatment groups received low dose mecobalamin1.5 mg/kg, high dose of mecobalamin 2.5 mg/kg by oral route for 10 days. Upon completion of the treatment period kidney tissues were taken and kidney injury was assessed glutathione, protein content (BCA assay) as well as pro-inflammatory cytokines TNF-α using ELISA. The results from the follow up tissue sample analysis following the completion of the cisplatin protocol demonstrated significantly increased levels of glutathione and TNF-α in the mice that were challenged with cisplatin alone, indicating acute kidney injury ($p < 0.05$). In regards to mecobalamin 2.5 mg/kg treatment had significantly lower kidney damage markers compared to both mecobalamin 1.5 mg/kg and silymarin treatments ($p< 0.05$). These preliminary findings suggest that mecobalamin could potentially be used as supportive treatment in cisplatin induced nephrotoxicity injury.

Contents

List of Figures

List of Tables

Abbreviations

AG	Aminoglycosides
AIF	Apoptosis-Inducing Factor
AKI	Acute Kidney Injury
ALT	Alanine Aminotransferase
AST	Aspartate Aminotransferase
ATP	Adenosine Triphosphate
AVP	Arginine Vasopressin
BCA	Bicinchoninic Acid
BUN	Blood Urea Nitrogen
CAT	Catalase
CDDP	Cis-Diamminedichloroplatinum (Cisplatin)
CKD	Chronic Kidney Disease
CTR1	Copper Transporter 1
CYP450	Cytochrome P450
DMSO	Dimethyl Sulfoxide
DNA	Deoxyribonucleic Acid
ELISA	Enzyme-Linked Immunosorbent Assay
ER	Endoplasmic Reticulum
ERS	Endoplasmic Reticulum Stress
FAS	First Apoptosis Signal
GFR	Glomerular Filtration Rate
GSH	Glutathione
HO-1	Heme Oxygenase-1

IL-1	Interleukin 1
iNOS	Inducible Nitric Oxide Synthase
IP	Intraperitoneal
KIM-1	Kidney Injury Molecule 1
MAPK	Mitogen-Activated Protein Kinase
MCP-1	Monocyte Chemoattractant Protein-1
MRP	Multidrug Resistance Protein
NAC	N-Acetylcysteine
NADPH	Nicotinamide Adenine Dinucleotide Phosphate
NF-κB	Nuclear Factor Kappa B
NOX	NADPH Oxidase
OCT2	Organic Cation Transporter 2
PBS	Phosphate Buffered Saline
PPE	Personal Protective Equipment
Prx I	Peroxiredoxin I
ROS	Reactive Oxygen Species
SCr	Serum Creatinine
SMAC/DIABLO	Second Mitochondria-Derived Activator of Caspases
SOD	Superoxide Dismutase
TNF-α	Tumor Necrosis Factor Alpha

Symbols

C	Degrees Celsius (temperature)
μL	Microliter (volume)
μM	Micromolar (concentration)
μg	Microgram (mass)
μmol	Micromole (amount of substance)
g	Gram (mass)
kg	Kilogram (mass)
mg	Milligram (mass)
mg/kg	Milligrams per kilogram (dose)
mL	Milliliter (volume)
mol/L	Molarity (moles per liter)
n	Number of samples (e.g., n = 6 mice per group)
p	p-value (statistical significance)
pH	Power of Hydrogen (acidity/basicity)
TNF-α	Tumor Necrosis Factor-alpha
$\uparrow$	Increased (e.g., $\uparrow$ TNF-α level)
$\downarrow$	Decreased (e.g., $\uparrow$ GSH level)

Chapter 1

Introduction

1.1 Kidney

Waste products and toxins such as urea, creatinine, and uric acid must be removed by the kidneys. They produce hormones such as erythropoietin, vitamin D, and renin, and regulate serum osmolality, electrolyte levels, and extracellular fluid volume [1].

The kidney regulates electrolyte and water balance, acid-base levels, blood pressure, hormone secretion, and waste removal. Mammalian kidneys house at least 16 distinct, highly specialized epithelial cell types, alongside diverse immune cells, endothelial cells, and interstitial cells. This intricate cellular network requires precise coordination for proper kidney function [2].

Historically, kidney cells were classified based on microscopic appearance and function. However, the emergence of single-cell techniques—like transcriptomics, epigenetics, metabolomics, and proteomics—has revolutionized cell characterization, enabling more precise classification and deeper functional insights into renal cells [3].

1.2 Functional Unit of Kidney

The functional unit of the mammalian kidney is the nephron. It comprises the filtering glomerulus connected to a long, segmented tubule. This tubule has distinct regions: the proximal tubule reabsorbs vital nutrients, an intermediate segment (like the loop of Henle) controls osmolarity, and the distal tubule regulates electrolyte balance and performs final adjustments. The tight-knit network of immunological, endothelial, interstitial, and epithelial cells is necessary to achieve maximum function [4].

There are cortical medullary spatial differences in addition to proximal-distal regional differences. The medullary region is hypoxic even at resting levels, and the cortex and medulla have significant differences in interstitial sodium and urea concentrations that are essential for maintaining water homeostasis. To survive in such an environment, specialized immune and epithelial cells are required [5].

There are two capillary beds in the kidney. One of the main forces behind filtration is the ability of glomerular capillaries, which emerge from the afferent arterioles, to tolerate high hydrostatic pressures. The efferent arterioles receive the blood from the glomerular capillaries and then split off to form the peritubular capillaries, the second capillary bed. Fluid reabsorbed and electrolytes are returned to the circulation by this second capillary system, which has a low hydrostatic pressure. The kidney can rapidly adjust to changes in the environment and decouple glomerular filtration from variations in blood pressure by altering the diameter of the afferent and efferent arteries [6]. The advent of high-throughput single-cell transcriptomics allows simultaneous interrogation of the whole transcriptome in thousands of individual cells. Subsequent clustering analysis organizes cells based on global gene expression similarity, offering a powerful, albeit resolution-sensitive and potentially capture-biased, method for cell classification. Application of these techniques to the kidney has yielded a gene expression-derived cell type atlas that closely aligns with classical functional and genetic characterizations. Each renal cell type possesses a unique transcriptional identity evolved to support its specific role within the nephron. Leveraging single-cell multi-omics data, researchers are now dissecting the mechanistic links between cell-specific gene expression and function, characterizing

transcriptional plasticity during disease states and adaptive processes, and mapping the complex cellular crosstalk critical for renal homeostasis [7].

1.3 The Complex Vasculature of the Kidney

The human kidneys receive more than 20% of the cardiac output despite only weighing 100–180 g (0.5% body weight). Because the arterial system produces two successive capillary beds, the kidneys' circulation is complicated. It feeds the glomerular capillary bed by first branching into the afferent arterioles of the glomerulus. The efferent arteriole then branches again to create the peritubular capillary bed, which supplies the entire nephron. Because of their close proximity to the tubular epithelial cells, peritubular capillaries are essential for reabsorption, while glomerular capillaries are essential for producing the primary filtrate [8].

There are many endothelial cells in the kidney. Even in the first whole kidney single-cell sequencing analysis, glomerular and pericapillary endothelial cells can be distinguished from one another. Sorting-based enrichment has now been used in a number of studies to conduct single-cell analysis that is solely focused on renal endothelial cells [9].

For filtration, glomerular endothelial cells are essential. They differ greatly from other endothelial beds in the body because they are fenestrated. A double capillary bed system is part of the kidney's intricate vascular system; the first glomerular capillary bed regulates filtration, while the second peritubular capillary system is crucial for reabsorption [10].

1.4 Nephrotoxicity

The structural damage to the kidneys and the decline in kidney function that follows the use of different medications is referred to as nephrotoxicity. Drug nephrotoxicity is divided into two primary categories: idiosyncratic toxicity and dose-dependent toxicity. Acute kidney injury (AKI), the third primary cause of drug toxicity, is one of the various ways

that kidney damage can appear after the administration of a nephrotoxic medication. Chemotherapeutic drugs are frequently linked to an acute decrease in glomerular filtration rate [11].

One of the most common adverse effects of chemotherapy with different medications is nephrotoxicity. Acute kidney injury (AKI) affects roughly 13.3% of people worldwide each year, making it a massive global health concern. Although the pathophysiology of AKI is extremely complicated, ischemia, nephrotoxicity, and sepsis are its primary causes. Drug use is primarily linked to nephrotoxicity. AKI caused by drugs is responsible for 19–26% of all hospitalized cases [12]. Done of the three mechanisms described below describes how nephrotoxicity arises due to drug toxicity:

1. Apical contact with drugs or their metabolites, drug and metabolite transport from the apical surface, and drug release from the basolateral surface into the tubular lumen are the mechanisms that lead to proximal tubular damage and ATN (a dose-dependent process).

2. Tubular obstruction also show dose dependent mechanism caused by crystals or casts containing medications and their metabolites.

3. Drugs and their metabolites can cause interstitial nephritis (a mechanism that is independent of dosage) [13].

Glomerular filtration rate shows a sharp decline is referred to as acute kidney injury (AKI), formerly known as acute renal failure. Currently, it is defined as a 50% relative increase over 48 hours.AKI affects roughly 13.3 million people worldwide each year, making it a massive global health concern. Twenty to sixty percent of critically ill patients develop AKI, making them the group most affected by this condition [14].

1.4.1 Mechanisms of Nephrotoxicity

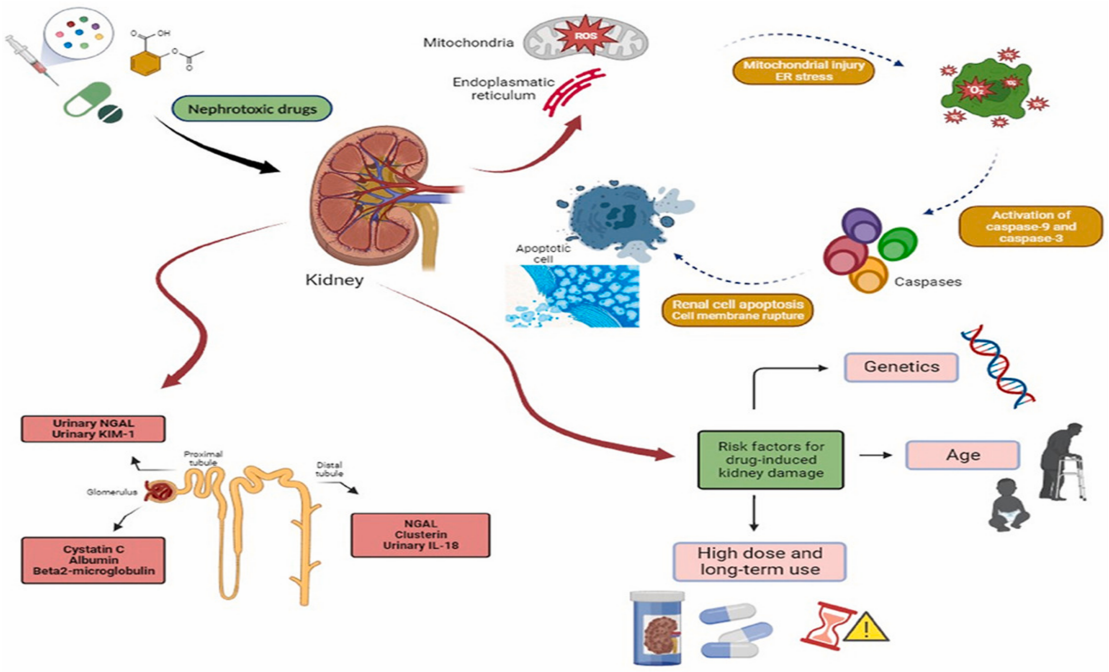

FIGURE 1.1: Graphical representation of pathways involved in nephrotoxicity; Drug induced damage, genetics ,age ,Nephrotoxic drugs high dose and long term use.

The kidneys, gastrointestinal system, and liver all metabolize drugs. There are two pathways for the excretion of drugs and their metabolites: extrarenal and renal. With an emphasis on renal excretion, medications can be eliminated through tubular secretion or glomerular filtration. The tubules and the surrounding interstitium are exposed to potentially harmful substances along each excretion pathway. Through apical contact with the substances secreted into the tubular lumen, their absorption by the tubular epithelial cells, or their apical efflux from the peritubular circulation (the basolateral regions of the tubular cells) into the tubular lumen, the (primarily proximal) tubules are made visible. The compounds are transported from the proximal tubule (PT) into the loop of Henle and subsequently into the distal tubule by tubular secretion and glomerular filtration. Drugs may precipitate, crystallize, or form casts in the more distal tubules, causing tubular obstruction. Interstitial nephritis, which is caused by tubulointerstitial inflammation, is another mechanism [15].

1.4.2 Tubular Epithelial Injury via Apical Contact with Drugs or via Uptake of Drugs

The PT receives all substances that are filtered by the glomerulus. They may be harmful to the tubular epithelium, even if a sizable portion of them are absorbed by it. The proximal tubule (PT) reabsorbs a wide range of substances, including drugs (e.g., aminoglycosides, AGs), sugars, and heavy metals. AGs represent a prototypical cause of PT injury. Nephrotoxicity occurs in 10-25% of patients receiving AG therapy. The most common clinical manifestation is a polyuric acute kidney injury (AKI), characterized by elevated serum creatinine, impaired urinary concentrating ability, and features of proximal tubular dysfunction. These features include glycosuria, enzymuria, aminoaciduria, and electrolyte wasting (hypercalciuria, hypermagnesuria, hypocalcemia, hypomagnesemia). AGs are selectively taken up by PT cells via receptor-mediated endocytosis, primarily through the apical megalin-cubilin complex. Following endocytosis, AGs accumulate within subcellular compartments, including the Golgi apparatus, lysosomes, and endoplasmic reticulum (ER). This accumulation is facilitated by the electrostatic interaction between the cationic AG molecules and the anionic phospholipids present in cellular and organellar membranes [16].

AG-induced phospholipidosis, characterized by impaired degradation due to inhibition of lysosomal phospholipases (A1, A2, C) and altered phospholipid charge, exacerbates AG uptake and is a key determinant of nephrotoxicity severity. When AG concentrations exceed a critical threshold within intracellular compartments, organellar membranes rupture, spilling contents into the cytosol. Cytosolic AGs then directly impair mitochondrial function, disrupting the respiratory chain. This results in ATP synthesis failure and excessive ROS production, culminating in cell death via apoptosis or necrosis. Concurrently, AGs stabilize the pro-apoptotic regulator Bax by inhibiting its degradation, amplifying the apoptotic signal. The protease cathepsin, which is activated by cytoplasmic lysosomes, either directly or indirectly destroys cells by inducing caspase activation, which in turn causes apoptosis [17].

AGs inhibit membrane transporters in both the apical and basolateral membranes, regardless of the mechanism of injury. It has been demonstrated that they block the activity of the Na-Pi cotransporter, Na-H exchanger, carrier-mediated dipeptide transporter, electrogenic Na transporter, and Na-K ATPase. This disrupts reabsorption by increasing ion excretion and damages the cell's ability to maintain electrolyte and water homeostasis, which leads to swelling and eventual death. Instead of binding to the megalin-cubilin receptor, polysaccharides and starch used in infusion fluids are pinocytosed, accumulate in lysosomes, inhibit their enzymes, rupture their membranes, and release their contents into the cytoplasm. Their accumulation results in lumen occlusion and swelling of epithelial cells because of their osmotically active nature. We call this kind of damage osmotic nephropathy [18].

1.4.3 Proximal Tubular Injury via Drug Secretion from the Basolateral Surface into the Tubular Lumen

Certain medications are eliminated through tubular secretion; this process initiates in the peritubular capillaries. Molecules pass across the basolateral membrane of renal tubular epithelial cells via specific transporters and then enter the tubular lumen via the apical side. For example, organic cations can be transported on the basolateral side via human organic cation transporter (hOCT) and organic anions are absorbed via human organic anion transporter (hOAT). The transporters deliver the molecules to the tubular cell's apical membrane, where various efflux transporters, such as P-glycoprotein (P-gp), multidrug resistance-associated proteins (MRPs), and multidrug and toxin extrusion protein 1 (MATE1), transport them into the proximal tubular lumen. If those potentially toxic molecules begin to stay within the tubular cells, they can cause cellular damage. This can occur when efflux transporter mutations occur or when other endogenous or exogenous substance inhibit efflux transporters. A different scenario occurs when a drug is in large excess in blood and peritubular circulation, which leads to unnecessary basolateral transport and drug accumulation in the cytoplasm. Cisplatin and tenofovir cause injury to PTs. Tenofovir treats hepatitis B and Human Immunodeficiency Virus (HIV) [19].

Nephrotoxicity can arise through a number of mechanisms, such as direct cytotoxicity to the tubular epithelial cells, oxidative stress, DNA adducts, inflammation, and mitochondrial dysfunction. Endoplasmic reticulum stress, mitochondrial dysfunction, oxidative stress, immune complement activation, and caspase protein activation are the pathways that contribute to nephrotoxicity. An imbalance between pro-oxidant and antioxidant mechanisms is known as oxidative stress. An increase in reactive oxygen species (ROS) is the main cause of the nephrotoxic effects.

1.5 Cisplatin

Cisplatin is an antineoplastic agent that contains platinum and has shown promise in treating a number of cancer types. By stopping the cell cycle and altering DNA synthesis, cisplatin causes cancer cells to undergo apoptosis. Cisplatin is regarded as a first-line treatment for cancers of the head, neck, bladder, and lungs.Cisplatin, sometimes referred to as cis-diamine-dichloro-platinum (II) or CDDP, forms intra- and inter-strand crosslinks and covalently binds to purine DNA bases to produce its non-cell-cycle specific cytotoxicity. After local DNA denaturation, strand breaks are ultimately caused by cellular repair mechanisms. Although many of these strand breaks can frequently be repaired by excision repair enzymes, lingering damage to proteins, RNA, and DNA can cause cellular death through either apoptotic or non-apoptotic mechanisms [20].

By producing reactive oxygen species (ROS), cisplatin causes oxidative stress. The primary enzyme source of ROS in cisplatin nephrotoxicity, also referred to as NOXs, is NADPH oxidase, which is crucial for preserving cell homeostasis. NADPH is crucial for preventing the oxidation of glutathione (GSH) and for preserving the amount of intracellular reduced GSH. It is important to remember that renal cells are the primary source of NOX4 (NADPH Oxidase 4) expression. This suggests that NOX4 is essential for renal damage brought on by cisplatin. A specific antidote for cisplatin does not exist. Important management strategies and methods to lower toxicities include renoprotection, enhancing drug clearance with intense intravenous hydration with or without the use of an osmotic diuretic, and avoiding nephrotoxic medications [21].

1.5.1 Structural Alterations in Cisplatin-Associated Nephrotoxicity

From a clinical standpoint, differences in doses of cisplatin can lead to differences in nephrotoxicity. For instance, large doses, or multiple doses of cisplatin, can result in irreversible renal failure, whereas a single dose of cisplatin may result in reversible renal impairment. Pharmacokinetics studies demonstrate that the major contributors to nephrotoxicity are the large volume of cisplatin distribution and the long-term retention of cisplatin within the kidney. To summarize, the histopathological mechanisms of cisplatin-induced nephrotoxicity typically appear as ischemia (lack of blood supply) or necrosis (cell death) of proximal renal tubular epithelial cells and reductions in renal blood flow and glomerular filtration rate (GFR). The histopathology of cisplatin-induced nephrotoxicity is positively correlated with cisplatin dose. First, organic cation transporter 2 (OCT2) allows cisplatin to cross over time into the renal tubular cells passively and forms hydrates with adjacent water molecules, leading to relentless accumulation in renal cells. This process of the formation of cisplatin hydrate is reversible; this hydrate can disengage from cells if the hydrate dissociates into cisplatin and water molecules. Therefore, renal retention of cisplatin results in oxidative stress, autophagy, apoptosis, and DNA damage. As well, renal tubular epithelial cells lose their brush border due to cisplatin exposure [3].

Numerous immune cells, including T cells, dendritic cells, and macrophages, are drawn to damaged renal tubular epithelial cells and release a range of inflammatory factors. Furthermore, cisplatin can worsen tubular cell damage and decrease medullary blood flow, which can result in acute ischemic kidney injury. Cisplatin-induced AKI causes obvious vasoconstriction in place of the normal self-regulatory renal vasodilation in ischemic kidneys, which can result in hypoxic injury and, in extreme situations, vascular injury. According to certain research, cisplatin combines with reduced glutathione in the liver before moving on to the kidney. Glutamyltransferase in the brush edge of the renal proximal tubule breaks down cisplatin into a nephrotoxic metabolite, which results in renal cell necrosis or apoptosis [22].

1.5.2 Mechanismsof Cisplatin-Induced Nephrotoxicity

Severe side effects, such as nephrotoxicity, ototoxicity, neurotoxicity, and vomiting, frequently restrict the use of cisplatin chemotherapy. phrotoxicity limits the clinical utility of cisplatin, caused by linked factors including oxidative injury, apoptotic cell death, inflammatory mediators, and decreased autophagy. Understanding the background pathophysiology is important for mitigation.

Cisplatin is primarily renally excreted leading to significant accumulation in renal tubular cells. This is mediated by uptake by multiple transporters, including OCT2 (SLC22A2) and CTR1 (SLC31A1), in addition to passive diffusion. All of these components combine all of the components of glomerular filtration, tubular secretion and reabsorption, and uptick via transporters that concentrate intracellular levels to toxic levels.

Furthermore, multidrug and toxin extrusion 1 and solute carrier family 47 member 1 secrete cisplatin into the lumen. The nephrotoxicity caused by cisplatin can be considerably decreased by knocking down the Oct2 gene.

Patients with Oct2 mutations consistently exhibit decreased cisplatin transport into renal tubular cells and low OCT2 expression, which reduces nephrotoxicity. Furthermore, cisplatin uptake and the ensuing cytotoxicity are considerably reduced when CTR1 expression is downregulated.

Furthermore, mice lacking peroxiredoxin I (Prx I) exhibit greater resistance to cisplatin-induced nephrotoxicity compared to wild-type mice. This is because Prx I-deficient mice exhibit elevated excretion of cisplatin through the high expression of renal efflux transporters multidrug resistance-related protein 2 (MRP2) and MRP4 [23].

1.5.3 DNA Damage

Cisplatin binds to DNA to create adducts that damage DNA, which is how it mediates its cytotoxic effects. Water molecules take the place of cisplatin's chloride ligand in an aqueous environment to create a positively charged hydrated complex ion, which is then

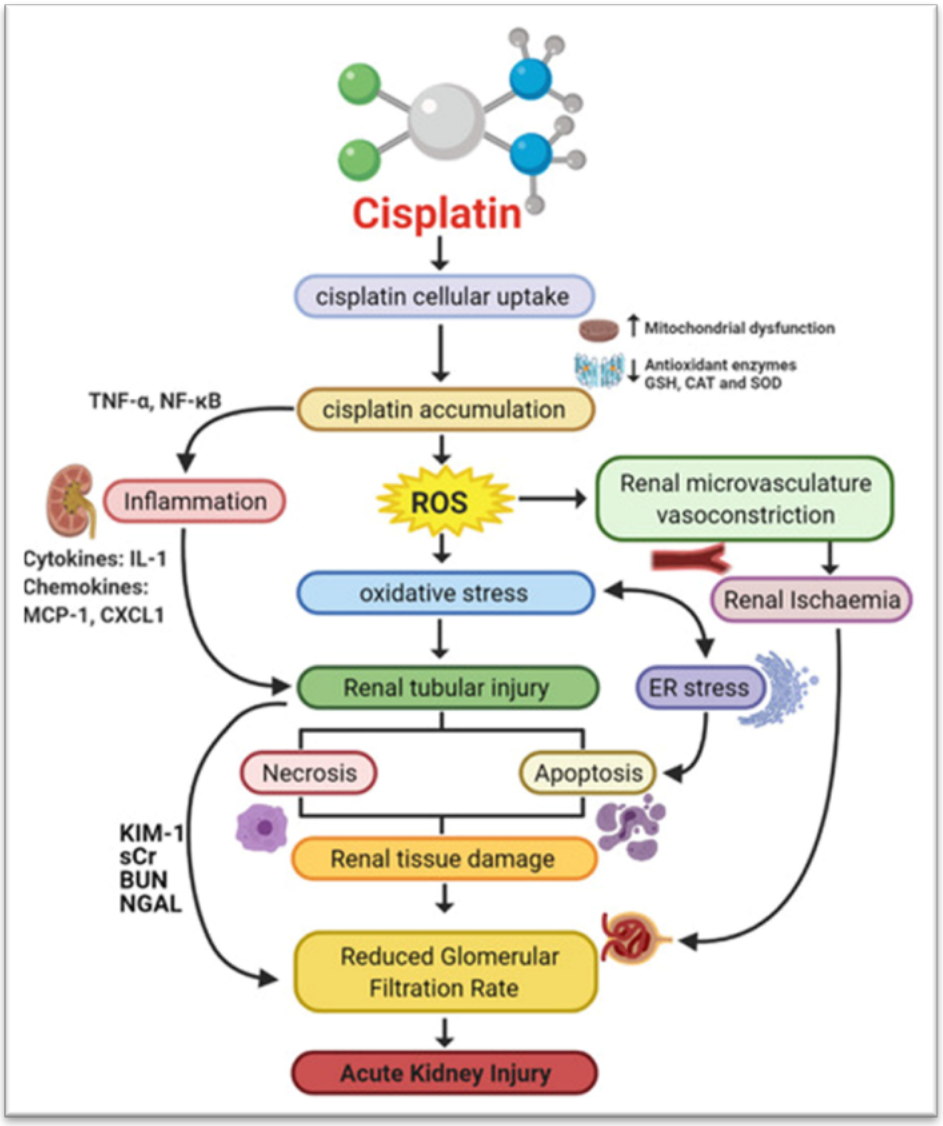

FIGURE 1.2: Detrimental nephrotoxic effect of cisplatin in renal tissue

drawn to the nucleus by DNA electrostatic attraction. Then, in rapidly proliferating cells, this complex binds to DNA to form an adduct, which causes DNA cross-linking and inhibits DNA synthesis and replication.

This phenomenon is pronounced in cells with defective DNA repair. Less than 1% of platinum binds to nuclear DNA, while cisplatin binds to it nonspecifically. It's interesting to note that mitochondrial DNA is more vulnerable to cisplatin-mediated cytotoxicity than nuclear DNA. The hydrolysis of cisplatin results in the production of positively charged metabolites, which preferentially gather in negatively charged mitochondria.

Thus, mitochondrial density and mitochondrial membrane potential in cells determine how sensitive cells are to cisplatin. The renal proximal tubule is the kidney's most sensitive site to cisplatin because it contains areas with a relatively high mitochondrial density [23].

1.5.4 Apoptosis

According to reports, renal tubular epithelial apoptosis is caused by a low concentration of cisplatin (8 μM), whereas necrosis is induced by a high concentration of cisplatin (800 μM). Endoplasmic reticulum stress (ERS) pathways, death receptor-mediated exogenous pathways, and mitochondria-mediated endogenous pathways are the main pathways linked to cisplatin-induced apoptosis in renal tubular cells [23].

1.6 Mitochondria - Mediated Endogenous Pathways

Cisplatin causes mitochondrial apoptosis via caspase-dependent and -independent pathways. Once cisplatin enters renal tubular epithelial cells, it facilitates BAX's translocation to the mitochondria, with subsequent activation of caspase-2 and the release of cytochrome c, SMAC/DIABLO (second mitochondria-derived activator of caspases/direct IAP-binding protein with low isoelectric point), HtrA2/Omi (high temperature requirement protein A2), and apoptosis-inducing factor (AIF) from the mitochondria. The release of these factors then activates caspase-9 to ultimately execute apoptosis [23].

1.7 Death Receptor-Mediated Exogenous Pathways

Cisplatin activates caspase-8, which in turn activates caspase-3, which in turn triggers apoptosis, through binding to death receptors on the cell membrane, including tumor necrosis factor receptor 1 (TNFR1), TNFR2, and FAS. Tumor necrosis factor-α (TNF-α) is upregulated by cisplatin, which facilitates the interaction between TNF-α and TNF

receptors, such as TNFR1 and TNFR2. TNFR1 can directly induce exogenous apoptosis and possesses a death domain.

However, because it lacks a death domain, TNFR2 primarily controls the inflammatory response to trigger apoptosis. Although the precise mechanisms are still unknown, cisplatin can also activate the FAS/FAS-L system, and the FAS-associated death domain further interacts with FAS or TNFR1 to induce apoptosis [24].

1.8 Endoplasmic Reticulum Stress Pathways

Cisplatin is known to also activate the endoplasmic reticulum stress (ERS) directed apoptotic pathway. Once cisplatin enters the cell it becomes intracellularly modified and disrupts the function of cytochrome P450 (CYP450) on the endoplasmic reticulum membrane that results in oxidative stress and activation of caspase-12 to induce apoptosis. Studies on Cyp2e1 knockout mice have shown a significant decrease in cisplatin-mediated apoptosis which shows the influence of this enzyme. Furthermore, studies performed in rats demonstrated increased expression of ER stress and apoptotic markers (X-box binding protein 1), increases in calpain products, and elevated levels of cleaved caspase-12 products in kidney tissue following cisplatin administration [24].

1.8.1 Oxidative Stress

New studies have indicated that oxidative/nitrosative stress plays a key role in cisplatin nephrotoxicity, reflected by increased lipid peroxidation (MDA), DNA damage (8-OHdG), protein nitration (3-NT), and reduced overall antioxidant capacity (decreased SOD/CAT activity), which will contribute significantly towards our mechanistic understanding about the usefulness of antioxidants and ROS scavengers. Cisplatin appears to bind to and inactivate critical renal cytoprotective thiols, such as glutathione and metallothionein, after cellular entry to include acute depletion. ROS levels are also raised as a result of the inhibition of certain antioxidant enzymes, including glutathione reductase, SOD, and glutathione peroxidase. Adenosine triphosphate depletion results from ROS's impact on the

activity of mitochondrial complex enzymes I–IV, which prevents the oxidative respiratory chain from normally transmitting. Increased ROS then causes lipid peroxidation, which modifies the permeability and structure of membranes and further impairs cellular function. Lastly, ROS damage proteins, carbohydrates, and amino acids, which encourages apoptosis and DNA damage. Furthermore, elevated ROS can cause FAS-L, FAS, TNFR1, and TNF-α expression to rise, which ultimately leads to apoptosis [24].

1.8.2 Inflammation

The inflammatory response is linked to cisplatin-induced nephrotoxicity. A cisplatin-induced nephrotoxic mouse exhibits elevated renal TNF-α expression, and TNF-α inhibition or knockout can significantly reduce cisplatin-induced renal insufficiency and damage, suggesting that elevated TNF-α expression is a key factor in cisplatin-induced nephrotoxicity. It's interesting to note that TNF-α in the blood and urine following cisplatin administration might originate from renal epithelial cells rather than immune cells. Additionally, TNF-α triggers the generation of ROS, which further activates nuclear factor kappa light-chain-enhancer of activated B cells (NF-κB), a transcription factor that triggers the production of proinflammatory cytokines like TNFα. Mice's kidney function is improved when NF-κB transcriptional activity is inhibited by JSH-23, a type of NF-κB inhibitor.

TNF-α causes oxidative stress by activating chemokines and proinflammatory cytokines, which worsens kidney damage. Cisplatin-generated hydroxyl free radicals play a role in the regulation of TNF-α synthesis and the phosphorylation of p38 mitogen-activated protein kinase (p38 MAPK), which in turn triggers the activation of NF-κB. Thus, in the kidneys of mice, the hydroxyl radical scavenger dimethyl thiourea suppresses the activation of p38 MAPK and the expression of TNF-α mRNA. Inhibiting p38 MAPK effectively prevents cisplatin-induced kidney damage by lowering TNF-α production. Cisplatin-induced nephrotoxicity is also linked to other cytokines, including transforming growth factor-β, monocyte chemoattractant protein1 (MCP-1), intercellular adhesion molecule, and heme oxygenase-1 (HO-1). In order to protect the kidneys, the antioxidant N-acetylcysteine

(NAC) efficiently suppresses inflammation and complement system activation. O2– is produced by mitochondrial dysfunction, whereas TNF-α, nicotinamide adenine dinucleotide phosphate oxidase, and inducible nitric oxide synthase (iNOS) are all upregulated during the inflammatory response brought on by cisplatin, which directly results in the production of NO–. Apoptosis and necrosis are further induced by ONOO–, which is produced by NO– and O2– and has potent oxidation and nitration properties [24].

1.8.3 Autophagy

In order to preserve cellular homeostasis and endure cisplatin-induced nephrotoxicity, autophagy is crucial. Autophagy mediates cell damage, as evidenced by the inhibition of both apoptosis and autophagy increases in NRK-52E cells treated with cisplatin following beclin-1 knockdown. Another study, however, demonstrated the protective role of autophagy in cisplatin-induced kidney injury by demonstrating that autophagy inhibition accelerated apoptosis [24].

1.8.4 NADPH

Tumor cells heavily utilize their metabolic pathways to guarantee a sufficient supply of antioxidant molecules (such as GSH and NADPH) and control the synthesis of antioxidant enzymes in order to prevent excessive oxidative stress. A portion of the energy substrates used in these pathways can also be diverted to particular pathways that generate redox cofactors like NADH, which are necessary to preserve or restore proper redox homeostasis, in addition to antioxidant molecules like NADPH and GSH. One important aspect of cellular metabolism that is essential for cancer cells is the pentose phosphate pathway. PPP's ability to prevent cell death may be its most useful role in carcinogenesis.

To keep cancer cells' high proliferative advantage in the tumor environment, ROS produced by accelerated metabolism, hypoxia, or DNA damage must be controlled. By boosting the intracellular redox capacity of cancer cells through increased NADPH production, oxidative activation of PPP may aid transformed cells in avoiding oxidative

stress. increase in the production of the NADPH cofactor in tumor cells in comparison to the surrounding tissue using a technique we developed for in vivo optical biopsy. Our results are in line with data showing that elevated NADPH synthesis lowers intracellular ROS levels in HCC. One frequent genetic change in HCC is the activation of the Akt pathway, which can affect glucose metabolism and possibly NADH and NADPH levels. Increased NADH production may result from the promotion of glucose uptake and glycolysis by Akt activation. Additionally, PPP activity, which produces NADPH, may be increased by Akt signaling. Similarly, cellular metabolism and redox balance are impacted by loss of p53 function, another genetic change seen in HCC. The antitumor protein plays a role in controlling oxidative phosphorylation and glycolysis. Increased glycolysis from its deactivation may raise NADH levels. Furthermore, p53 affects the expression of genes that generate NADPH, like G6PD, which may have an effect on NADPH levels.

As an antioxidant, GSH plays a crucial role in preserving cells' normal redox state by preventing or reversing oxidative changes that cause mitochondrial dysfunction and cell death. GSH is significant due to its chemical versatility as well as its quantity. interaction with different types of ROS [25].

1.9 Silymarin

An extract from milk thistle called silymarin has anti-inflammatory, immunomodulatory, anti-lipid peroxidative, antifibrotic, anti-oxidative, and anti-proliferative qualities [26]. By focusing on a wide range of molecules, silymarin not only demonstrates anti-cancer properties by modifying several cancer hallmarks, such as cell cycle, metastasis, angiogenesis, apoptosis, and autophagy, but it also protects against toxicity brought on by chemotherapy, including nephrotoxicity, hepatotoxicity, cardiotoxicity, and neurotoxicity. Silymarin's poor water solubility, which results in low intestinal absorption and, consequently, low bioavailability, is one of its issues in (pre)clinical research. Silymarin nano formulations with extra advantages, such as superior drug loading, prolonged release, enhanced cellular uptake, and tumor cell targeting, have surfaced to address these

issues. In addition to its chemical and biological characteristics, we have outlined the anti-cancer properties and mechanism of action of silymarin in both free form and nano formulations and its protective roles against chemotherapy induced toxicity [27].

Nephrotoxicity is an expected adverse effect of chemotherapy resulting from structural injury to nephron components for drug filtering, detoxification, and excretion. Nephrotoxicity can also occur with more modern cancer treatments involving targeted therapy and immunotherapeutic agents, in addition to standard chemotherapy agents including methotrexate, cyclophosphamide, and cisplatin. Nephrotoxic effects can occur from intratubular obstruction, direct tubular cell toxicity, and changes to intrarenal vascular tone causing vasoconstriction. In vitro, silymarin's anti-apoptotic effect on tubular cells after cisplatin treatment was also verified. Furthermore, silymarin combined with other substances hastened the recovery of renal functions following chemotherapy-induced failure.

Research carried out a clinical trial study to ascertain the effects of silymarin (oral administration, 420 mg daily) on cisplatin-induced nephrotoxicity in humans, despite the fact that silymarin has nephroprotective qualities both in vitro and in vivo. Administering silymarin did not stop renal impairment and failure after receiving cisplatin. According to research silymarin's protective properties may be diminished by tablet formulation because of its extensive metabolism, low water solubility, low permeability across intestinal epithelial cells, and quick excretion in bile, receiving cisplatin-based chemotherapy showed improvements in kidney functions and a reduction in renal toxicity when silymarin and mesenchymal stem cells were combined to enhance the nephroprotective effects of silymarin.

Accordingly, alternative silymarin formulations and their combination with additional therapeutic and preventative agents are necessary for the protective effects of silymarin on chemotherapy-induced nephrotoxicity in humans [27].

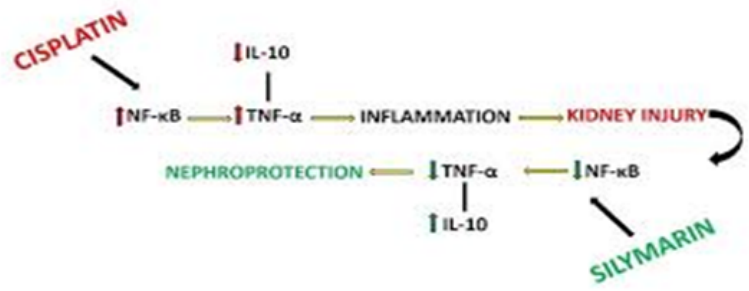

FIGURE 1.3: Mechanism of action of silymarin in CP-induced nephrotoxicity

Cisplatin (CP), an anticancer drug derived from platinum, is used to treat a variety of human cancers, including those of the brain, kidney, head, neck, lung, bladder, ovary, testicles, leukemia, and leukemia. Additionally, it is crucial in the management of germ cell cancer. It has side effects like neurotoxicity and ototoxicity, particularly neurotoxicity, despite its extremely potent anti-cancer effects. Renal dysfunction affected over 30% of CP patients. CP is still a commonly prescribed medication despite the fact that its harmful effects have been demonstrated. because it is a common medication used to treat head and neck cancer. Despite the complexity of the pathophysiology of acute kidney injury (AKI) brought on by CP, oxidative stress is the primary component [28].

Cytokines, particularly TNF-α, which in turn mediates inflammation. Pro-inflammatory cytokines IL1-β, MCP-1, and IL-6 are specifically activated by TNF-α, a strong cytokine that causes inflammatory tissue damage in the kidney. According to earlier research, CP triggers an inflammatory response by inducing the kidney to produce proinflammatory cytokines like TNF-α, IL-1β, IL-6, MCP-1, and NF-kB. Administration of CP has been shown to activate NF-kB, which in turn promotes the kidney's production of other proinflammatory cytokines like TNF-α. Additionally, it suppresses the expression of TNF-α by preventing the synthesis of IL-10. In addition to preventing the synthesis of inflammatory cytokines, IL-10 protects against tissue damage [29].

Antioxidants have recently been shown to have a nephroprotective effect by reducing inflammation and oxidative stress in CP-induced nephrotoxicity. Also found that curcumin treatment significantly reduced elevated NF-κB and TNF-α expressions in CP-induced kidneys and demonstrated a nephroprotective effect by upregulating IL-10 expression. Likewise, it was noted that quercetin treatment enhanced CP-induced inflammatory

markers like TNF-α, iNOS, and neutrophil infiltration . Like earlier research, the current study found that silymarin treatment significantly reduced the rise in NF-kB and TNF-α expression brought on by CP. However, silymarin treatment markedly increased the expression of IL-10 that CP had suppressed.

Our study's conclusions show that silymarin has an anti-inflammatory effect against cisplatin induced nephrotoxicity in mice.

Inhibiting elevated TNF-α is one of the most crucial strategies to avoid kidney damage brought on by CP. TNF-α has been shown to directly harm tubular and glomerular cells and trigger both internal and external apoptotic pathways. The kidney tissues of rats treated with CP showed histopathological alterations, including diffuse renal tubular necrosis, degeneration, and mononuclear cellular infiltration.

Additionally, they noted that silymarin can improve these structural alterations brought on by CP, making it a useful nephroprotective agent. Similarly, CP application led to kidney deterioration, including glomerular atrophy, dilated filtration gap, loss of brush border of proximal collecting tubules, hypertrophied podocyte pedicels, and tubular cell vacuolization. However, Silymarin treatment alleviated these alterations. According to estimates, the histopathological results of earlier research may have something to do with the inflammation brought on by CP. According to this study, elevated TNF-α, a crucial indicator of inflammation, can directly harm kidney cells. Furthermore, the present investigation shows that silymarin inhibits TNF-α expression and raises the expression of of TNF-α and increases the expression of IL-10 [30].

Furthermore, the current study shows that silymarin suppresses TNF-α expression while increasing IL-10 expression, a cytokine that is both anti-inflammatory and tissue-protective. It may also act as a protective agent for kidney tissue cells. This study is believed to corroborate earlier research in this regard.

This study's findings suggested that silymarin might have a renoprotective effect by lowering the elevated inflammation that the kidneys are induced to experience. The downregulation of TNF-α and NF-kB expression and the upregulation of IL-10 expression are thought to be the primary mechanisms underlying silymarin's renoprotective effects.

Consequently, silymarin is thought to have potential as a preventative measure against CP-induced nephrotoxicity [31].

1.10 Mecobalamin

Cobalamin, also known as vitamin B12, is a water-soluble vitamin that the body is unable to produce on its own. The core of vitamin B12's chemical structure is a cobalt ion, which forms a corrin ring with four nitrogen ions.

The nitrogen ion of the dimethylbenzimidazole molecule is bound by the lower ligand of the cobalt ion (beta). Four cobalamin analogs are produced when the cobalt ion's upper ligand (alpha) binds to distinct groups: cyanocobalamin, MeCbl, adenosylcobalamin (AdoCbl), and hydroxycobalamin (OHCbl).

Mecobalamin (methylcobalamin), a biologically active coenzyme form of vitamin B , serves as an essential cofactor for vitamin B_{12}-dependent methyltransferases. Its principal therapeutic applications are in managing hyperhomocysteinemia and peripheral neuropathy.

The circulation of MeCbl is the distribution of cobalamin in the bloodstream is influenced by three proteins: TC-I, TC-II, and TC-III. About 75–90% of circulating MeCbl binds to non-specific TC-I once it enters the bloodstream, while the remaining portion binds to TC-II with a high affinity to enter the cells. Cobalamin analogs are typically eliminated from the bloodstream and tissues by TC-III, which then transports them to the liver for bile elimination.

MeCbl excretion is via liver as liver stores between 0.5 and 5.0 μg of MeCbl per day from the vitamin that is consumed. The body then reabsorbs this stored vitamin, mostly in ileal enterocytes, after it is secreted in the bile. Feces are the main excretion of any unabsorbed MeCbl from food or bile, resulting in an estimated daily loss of 0.1% of the body's stores. Urine removes excess MeCbl from the blood, such as following an injection.

The activity of absorption-related enzymes and vitamin B12's ability to bind proteins during distribution and/or intercellular metabolism are both impacted by genetic abnormalities. Aspartate 757 or serine 810 mutations reduce the MeCbl cofactor's reactivity to the methionine synthase binding site.

MeCbl's cellular and molecular action; The cell's cobalamin is transformed into two coenzymes, MeCbl and AdoCbl. Throughout the body, MeCbl catalyzes methylation reactions. Cobalamin can carry out its essential functions as a coenzyme in a variety of enzymatic reactions thanks to these conversions. Methionine synthase, which is essential for converting homocysteine to methionine, uses MeCbl as a methyl donor. S-adenosyl methionine, a crucial methyl donor in a number of bodily methylation reactions, is subsequently produced from methionine.

By directly regulating the secretion of inflammatory cytokines like TNF-α, IL-6, epidermal growth factor, and neuronal growth factor, cobalamin and its different analog forms aid in the regulation of both acute and chronic inflammatory conditions. By influencing the activity of T lymphocytes and natural killer cells, cobalamin can also alter immune responses.

Targeting this essential component of pathophysiology, MeCbl is a promising therapeutic agent that could improve treatment options, maximize therapeutic outcomes, and reduce side effects. MeCbl decreases inflammation in the injured nerve area by controlling NFκB activity in immune cells and neurons. This lowers TNF-α, IL-1β, and IL-6 levels while raising IL-10 levels. Additionally, MeCbl regulates ganglionic and peripheral sensitization, which inhibits neuronal ion channel activation and influences nerve impulse transmission. It also affects the thickness of the myelin sheath and axonal development in remyelination. Through the activation of mTOR proteins, it controls neurite outgrowth and neuronal cell survival. Additionally, by inhibiting the Erk1/2 pathway in Schwann cells, MeCbl thickens and densifies the myelin sheath, leading to enhanced lipid and MBP syntheses [32].

Multiple studies point to a more efficient uptake of methylcobalamin by the body compared to cyanocobalamin and in turn presumably a greater formation of active vitamin

B12 coenzymes. Oral intake of methylcobalamin and cyanocobalamin results in similar amounts of cobalamin but methylcobalamin is retained in the liver to a greater degree. Once in circulation cobalamin will bind to 2 proteins transcobalamin (TC) and haptocorrin. TC, a 43 kDa non glycoprotein transfers cobalamin from the gut for transfer into circulation which will transfer to cells. Functioning biomarkers to evaluate vitamin B12 status in adult are total homocysteine (tHcy) and methylamalonic acid. Methylcoblamin will be excreted through urine and methylcobalamin urinary excretion is about a third of that of cyanocobalamin for the same dose, hence cellular uptake is significantly higher. Clinical studies suggest daily doses are effective 0.5 to 6 mg with the most effective benefits occurring at the higher doses. Methycobal has been used alone and in combination with other drugs to manage neuropathic pain [33].

Vitamin B12 supplementation may result in a number of negative side effects, including hypersensitivity reactions with varying symptom severity. Based on the information that is currently available, cobalamin hypersensitivity is more likely to occur following intramuscular or subcutaneous administration than following oral administration. Additionally, it appears that long-term cobalamin administration increases the risk of developing a vitamin B12 allergy, regardless of the chemical form of the vitamin. Despite being relatively uncommon, cobalamin hypersensitivity can have significant clinical implications. This is because a sizable portion of the population suffers from vitamin B12 deficiency, particularly the elderly and those with long-term illnesses that hinder their ability to absorb the vitamin.

Furthermore, there is no other treatment option and cobalamin supplemental therapy is long-term (often lifetime). These factors lead to the search for remedies that will enable the safe continuation of cobalamin deficient supplementation. Numerous procedures for cyanocobalamin desensitization have been proposed; these vary in terms of length, the dynamics of a steady dose increase, or the injection technique (subcutaneous or intramuscular). According to a study of the evidence currently available in this area, cyanocobalamin desensitization appears to be a successful method of achieving tolerance to vitamin B12, enabling long-term supplementing of this vitamin independent of the chemical form, dosage, frequency, or mode of delivery [34].

Mecobalamin has the potential to act as an analgesic by increasing the amount and the activity of noradrenaline and serotonin (5-hydroxytryptamine) in the descending inhibitory pain pathways, but how it acts as an analgesic remains unknown. Mecobalamin also plays a role in rebuilding damaged nerves in neuropathic pain syndromes. In addition, it is likely assisting with normal glutathione levels in cells because it is acting as a direct antioxidant. Furthermore, mecobalamin is acting as a reactive oxygen species (ROS) scavenger and preventing oxidative stress mediated activation of apoptosis transcript factors such as caspase-3 to protect against cell death. Its presence can also provide cellular protection by restoring the redox balance and lowering concentrations of TNF-alpha. Mecobalamin is known to be cobalamin (vitamin B12) and it is often celebrated as nature's most sophisticated cofactor, due to its biological role and molecular architecture [35].

Our study aims to evaluate the role of mecobalamin in cisplatin-induced Nephrotoxicity. To our knowledge, the mecobalamin effect on nephrotoxicity has not been assessed against cisplatin-induced nephrotoxicity.

Chapter 2

Literature Review

2.1 Epidemiological and Public Health Implications of Cisplatin-Induced Nephrotoxicity

Despite advances in oncology, conventional cytotoxic chemotherapy remains a cornerstone treatment for numerous malignancies. Among the most prevalent and severe adverse effects of these agents is acute kidney injury (AKI). Platinum-based compounds (e.g., cisplatin), alkylating agents, antimetabolites, and antitumor antibiotics exhibit significant nephrotoxic potential. The onset of AKI introduces substantial clinical risks, including elevated morbidity and mortality, prolonged hospitalization, treatment interruption or dose reduction, and potential need for renal replacement therapy—collectively compromising optimal oncological management [36].

Chemotherapy-induced AKI, defined by abrupt renal dysfunction, critically threatens patient survival, health outcomes, and therapeutic efficacy. Although aggressive intravenous hydration and forced diuresis are prophylactic strategies, they often fail to fully prevent AKI during chemotherapy. Contributory or exacerbating factors include intravascular volume depletion, sepsis, concomitant nephrotoxins, tumor lysis syndrome, and direct malignancy-related renal injury. Consequently, despite therapeutic innovations, cytotoxic chemotherapy remains indispensable for many patients.

Standard chemotherapy does not directly target malignant cells so it has often been thought to cause ”collateral” injury to the fragile renal environment which can cause oxidative stress, inflammation, and renal tubular injury. The principal cause of acute kidney injury (AKI) in standard chemotherapy is acute tubular injury (ATI) although the mechanism of renal injury varies by chemotherapy agent. For instance, thrombotic microangiopathy (TMA) is typically seen with antimetabolites and antitumor antibiotics and nephritis is typically associated with oxaliplatin. Experimental agents had a variety of mechanisms, including crystal deposition, altered intraglomerular hemodynamics, and vascular constriction [37].

There are several factors that influence a person's vulnerability to AKI caused by chemotherapy, but the two most prevalent ones are growing older and a rising drug concentration over time. As expected, AKI was significantly predicted by concomitant diseases, especially a history of renal impairment. Genetic diversity may have contributed to the increased prevalence of AKI by causing differences in the metabolism and transport of some medicines among individuals. Lastly, concurrent use of a diuretic or another nephrotoxic drug may further increase the risk.

Even while AKI brought on by chemotherapy is becoming more widely acknowledged as a serious clinical issue, prevention of this illness remains challenging. Intravenous (IV) hydration with isotonic saline is a typical method to prevent renal injury by maintaining appropriate urine production and volemic state.

2.1.1 Specialized Nephroprotective Strategies & Therapeutic Challenges

Adjunctive interventions for chemotherapy-induced nephrotoxicity are regimen-specific. Examples include sodium bicarbonate infusion for urine alkalinization and leucovorin rescue protocols during high-dose methotrexate or pemetrexed therapy. Investigative preventive measures, such as protein A immunoadsorption for mitomycin C-associated hemolytic-uremic syndrome, demonstrate limited clinical feasibility. The efficacy of other strategies, including mannitol diuresis for cisplatin, remains contentious [38].

2.1.2 Research Imperatives and Current Management Limitations

Despite the high incidence of chemotherapy-associated acute kidney injury (AKI), therapeutic options post-onset remain constrained. Current management is predominantly supportive, encompassing rigorous electrolyte correction and renal replacement therapy when indicated. Significant research efforts are directed at validating novel biomarkers for subclinical AKI detection to enable preemptive intervention. Key investigative priorities include elucidating pathophysiological mechanisms, identifying modifiable risk factors, refining early diagnostic modalities, and developing renoprotective strategies to mitigate nephrotoxicity and preserve glomerular filtration rate (GFR) [39].

2.1.3 Cisplatin: Clinical Utility and Nephrotoxic Burden

Cisplatin, an inorganic platinum-based chemotherapeutic alkylating agent, is widely employed against solid malignancies (e.g., lung, genitourinary, head, and neck carcinomas). Its primary antineoplastic mechanism involves intrastrand and interstrand DNA crosslinking with purine bases, inducing DNA replication arrest and apoptosis [40].

2.1.4 Pathophysiological Mechanisms

The nephrotoxicity of cisplatin, while incompletely elucidated, is primarily attributed to reactive oxygen species (ROS) generation coupled with depletion of endogenous antioxidants — notably reduced glutathione (GSH) in renal tubular epithelial cells. Concurrently, an inflammatory cascade marked by elevated TNF-α and proinflammatory cytokines potentiates tubular damage. Histopathological evidence confirms these processes induce necrosis, apoptosis, and degeneration within the tubular epithelium, predominantly affecting proximal convoluted tubules due to their heightened platinum accumulation. Renal vasoconstriction with reduced perfusion further exacerbates functional impairment [41].

2.1.5 Dose-Response Relationship & Risk Factors

Nephrotoxicity severity exhibits dose-dependence: single doses >100 mg/m^2, cumulative exposure, and peak plasma platinum concentrations >6 μg/mL correlate with elevated AKI incidence. Alternative weekly low-dose regimens demonstrate reduced nephrotoxicity versus traditional 3-weekly high-dose infusion while maintaining comparable progression-free survival. Established demographic and clinical risk modifiers include:

a) Advanced age

b) Female sex

c) Smoking history

d) Hypoalbuminemia

e) Comorbidities (metastatic disease, cardiovascular disease, diabetes mellitus, hypertension)

f) Chemotherapy-induced emesis

g) Potential ethnic susceptibility (e.g., heightened risk in African American populations)

Validated 9-variable predictive model incorporates age, smoking status, hemoglobin, leukocyte count, serum albumin, serum magnesium, hypertension, diabetes, and cisplatin dose. Genetic polymorphisms also influence susceptibility; notably, variants in *OCT2/SLC22A2* (encoding organic cation transporter 2, mediating cisplatin tubular uptake) confer reduced nephrotoxicity risk [40].

Standard prophylaxis involves intravenous isotonic saline (FDA-recommended: 1-2L pre-infusion). Emerging evidence supports shorter-duration, lower-volume hydration (1.9–4.3L over 4–5h) as superior to traditional high-volume protocols (4.5–7.8L over ≥24h) for nephroprotection. Post-infusion oral hydration shows outpatient potential but is limited by treatment-related anorexia.

Clinical exposure to nephrotoxicity manifests in both acute and chronic forms, one common agent being the chemotherapeutic agent cisplatin. Research from preclinical models has clearly defined the cellular and molecular mechanisms of nephrotoxicity produced by cisplatin, to include intracellular insults such as DNA damage, mitochondrial injury, oxidative stress, and endoplasmic reticulum insult. Nephrotoxicity produced by cisplatin is caused by a series of stress responses including inflammation, autophagy, cell cycle arrest, senescence, apoptosis, and programmed necrosis. Furthermore, we are beginning to uncover evidence of epigenetic changes that influence acute kidney injury and acute kidney problem associated with chronic renal disease produced by cisplatin. More detailed understanding of the interconnectedness of these pathways, and the specific influence of cell types with regards to certain key mediators of controlled inflammation, necrosis, and epigenetic modifications in cisplatin nephrotoxicity are warranted. There are many potential therapeutic targets in reprimanding cisplatin nephrotoxicity. It is important to investigate the effect of any Reno protective strategy on the efficacy of cisplatin treatment. Additional exploration with the use of tumor bearing animals, multi-omics, and genome wide association studies will be necessary to understand the complexity of the physiological and molecular reasons for nephrotoxicity produced by cisplatin. If successful, the results of this study could be useful in identifying targets for kidney protection without the need to forego the nephrotoxic effects of cisplatin [42].

The polyphenolic flavonoid component silymarin, which is extracted from milk thistle (Sillybum marianum) seeds, has garnered attention due to its potent antioxidant, anti-inflammatory, and cytoprotective properties. Silymarin has been examined recently for its potential to reduce nephrotoxicity caused by cisplatin and other chemotherapy medications, although it has historically been used for hepatoprotection.

Silymarin is composed of flavonolignans, including silybin (the most active component), silydianin, and silychristin. Its ability to scavenge free radicals, improve endogenous antioxidant defenses like glutathione (GSH), superoxide dismutase (SOD), and catalase (CAT), and decrease lipid peroxidation are the main factors contributing to its therapeutic efficacy. Further altering inflammatory pathways, silymarin inhibits nuclear factor-kappa B (NF-κB) and tumor necrosis factor-alpha (TNF-α), two significant mediators of

renal inflammation and injury [43].

Cisplatin nephrotoxicity, associated with increased oxidative stress, apoptosis, and an intensified inflammatory response, leads to proximal tubular damage and lower renal function. The potential of silymarin to mitigate these effects has been the subject of numerous studies:

In preclinical studies, silymarin significantly reduces serum creatinine, blood urea nitrogen (BUN), and histological markers of tubular necrosis after cisplatin treatment. Malondialdehyde (MDA), a measure of lipid peroxidation, is reduced, while antioxidant enzyme levels are increased. In renal tissue, silymarin also lowers pro-inflammatory cytokines such as interleukin-6 (IL-6), TNF-α, and MCP-1.

Both in vitro and in vivo, silymarin's anti-apoptotic action demonstrated that it prevents cisplatin-induced apoptosis by stabilizing mitochondrial membranes, reducing caspase-3 activation, and preserving cellular integrity. It also promotes anti-apoptotic signaling pathways by upregulating Bcl-2 and downregulating Bax expression.

Improvements in histopathology reveal less tubular vacuolization, inflammatory infiltration, and degeneration in kidney tissues treated with silymarin. The material promotes brush border integrity and a healthy glomerular architecture.

Experimental models of kidney injury produced by cisplatin have demonstrated silymarin's significant nephroprotective advantages. Its antioxidant and anti-inflammatory properties help to lessen the primary pathogenic pathways that lead to nephrotoxicity. However, the limitations of its pharmacokinetic, formulation, and clinical data underscore the necessity of further research, particularly in human trials and in combination with more bioavailable or synergistic medications.

Mecobalamin (MeCbl), also known as methyl cobalamin, is the coenzyme form of vitamin B12 and is necessary for DNA synthesis, cellular methylation, and redox balance. Although mecobalamin has long been used to treat megaloblastic anemia and peripheral neuropathy, its broader cytoprotective, anti-inflammatory, and antioxidant properties earned interest in recent years. New experimental data indicates that it may be helpful in reducing kidney damage caused by inflammation and oxidative stress, particularly

when it comes to drug-induced nephrotoxicity, despite the fact that its nephroprotective action has not been thoroughly studied.

Methionine synthase, which helps produce S-adenosylmethionine (SAM), a universal methyl donor required for DNA repair and protein methylation, requires mecobalamin to remethylate homocysteine to methionine. This metabolic pathway is essential to sustaining genomic integrity and cellular defense mechanisms.

a) In renal pathophysiology, inflammation and oxidative stress are important contributors to tissue destruction. Mecobalamin reduces them by:

b) Enhancing methionine metabolism to increase glutathione (GSH) production.

c) Reducing reactive oxygen species (ROS) via scavenging free radicals.

d) Blocking tumor necrosis factor-alpha (TNF-α) and interleukin-6 (IL-6).

e) Promoting DNA repair and avoiding the death of kidney cells under stress.

All of these processes suggest that mecobalamin might have potent nephroprotective benefits. Several molecular mechanisms have been implicated in the protective effects of mecobalamin on the kidney: Antioxidant Action: One of the cellular antioxidant defenses that mecobalamin builds up is the creation of GSH, which is necessary for detoxifying ROS in renal tubular cells [44].

Anti-inflammatory Effect: It reduces the synthesis of pro-inflammatory cytokines by altering NF-κB activity, a crucial regulator in inflammation-driven nephrotoxicity.

By downregulating pro-apoptotic proteins (such caspase-3 and Bax) and upregulating anti-apoptotic proteins (like Bcl-2), mecobalamin prevents apoptosis and preserves the integrity of tubular epithelial cells. DNA Repair and Methylation: By supplying methyl groups via SAM, mecobalamin supports DNA integrity and repair in the face of oxidative stress.

Improved Redox Balance: Mecobalamin indirectly maintains NADPH levels through the methionine and folate cycles, which are essential for antioxidant renewal.

Advantages Mecobalamin offers several benefits over traditional nephroprotective antioxidants (such silymarin and N-acetylcysteine) when compared to other antioxidants.

a) It is water soluble and well tolerated, even at high dosages.

b) Improved intracellular retention and active transporting into renal cells.

c) Supporting both antioxidant defense and DNA methylation.

d) Long-term use is safe, especially for populations with subclinical B_{12} deficiency, which is common in patients with chronic illnesses and the elderly.

2.1.5.1 Objectives

a) To evaluate oxidative stress marker Glutathione reductase enzyme (GSR) in cisplatin-induced nephrotoxicity by spectrophotometry.

b) To Determine the histopathological changes in kidney enzymes Nicotinamide adenine dinucleotide phosphate oxidase (NADPH oxidase) in cisplatin-induced toxicity by using commercially available kits.

c) To investigate the role of cytokine TNF-alpha in cisplatin-induced nephrotoxicity by ELISA.

d) To Explore the potential anti-inflammatory effects of Mecobalamin against cisplatin-induced nephrotoxicity by ELISA.

Chapter 3

Materials and Method

3.1 Materials and Methods Ethics Statement

The experiment with animals was carried out per the approved guidelines. All experimental protocols were approved by the research and ethical committee (REC) of Capital University of Science and Technology, Islamabad. Protocol number REC/FOP/F2024/13, dated 06/09/2024)

3.2 Animal Handling

Four-week-old balb/c female mice weighing between 26 and 30 grams were acquired from Capital University of Science and Technology's local breeding facility in Islamabad. Mice were maintained in a controlled environment with a 12 hour light/dark cycle, maintained at a temperature of 22 $\pm$ 2 ^{o}C with a relative humidity of 50 $\pm$ 10% and were provided with a standard lab chow diet and water. Mice were acclimated to the lab prior to the start of the experiments for a period of seven days.

3.3 Intraperitoneal (IP) Route of Drug Administration in Mice

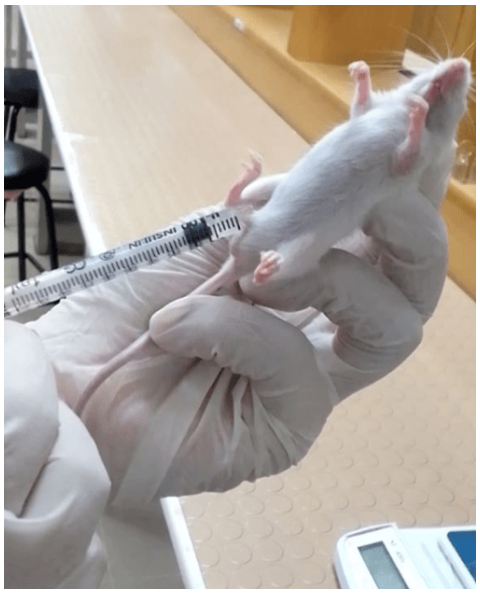

FIGURE 3.1: Figure, demonstrating appropriate administration of intraperitoneal injection in mice. Insert needle into lower right quadrant of the abdomen towards the head at 30-40 angle to horizontal.the speed of injection depends on the volume and viscosity of the substance.injection can be completed in 1-2 seconds. Pull the needle straight out and place the syringe into sharp container. Place the animal back into its cage and observe for any complications. Figure taken in Pharmacy department CUST university, Islamabad.

FIGURE 3.2: This figure shows the marking on tail of mice usig pen using and daily remarking of tail was done. Figure taken in Pharmacy department CUST university, Islamabad.

Animals can be administered intraperitoneally (IP) quickly and with little stress. In order to prevent unintentional penetration of the viscera, the rodent must be held supine with its head angled lower than the posterior portion of its body. The needle must then be inserted in the lower quadrant of the abdomen at an angle of about 10° [45].

3.4 Experimental Design

3.4.1 Randomized Control Method

A randomized controlled trial was a prospective, comparative, quantitative experiment conducted under controlled conditions and with random assignment of interventions to comparison groups. The randomized controlled trial was the most rigorous and rigorous research design for testing the existence of a causal effect relationship between an intervention and an outcome.

By using randomize control method mice were divided into five groups, Six mice in each group.

a) Group-1: Control group: mice received normal saline intraperitoneally (i.p)

b) Group-2: Cisplatin group: mice in this group received cisplatin (10mg/kg i.p single dose)

c) Group-3: Cisplatin and silymarin group (10mg/kg i.p and 50mg/kg orally for ten days)

d) Group-4: Cisplatin and Mecobalamin group (10mg/kg i.p and 1.5 mg orally for 10 days)

e) Group-5: Cisplatin and Mecobalamin group (10mg/kg i.p and 2.5 mg orally for 10 days)

The ethics Committee of the Faculty of Pharmacy, CUST had approved all animal protocols and experimental procedures.

3.5 Chemicals

All the drugs and chemicals used for the experiments were of standard analytical grade. Cisplatin was obtained from the Pharmedic and used to induce nephrotoxicity. Mecobalamin were obtained from Amson Vaccine and Pharma. Mecobalamin was used as treatment and silymarin used as standard drug.

3.6 Dosing Protocol

A 1 ml, 30 gauge BD Ultra-fine II insulin syringe was used. Appendruff tubes, weighing balances, and vortex mixers are some of the equipment used to formulate stock solutions. The drug was made fresh for everyday use.

The dosage was given to each mouse based on their body weight. To give the precise dosage, each mouse's weight was measured every day before the injection. Mice in the treatment group were given the drug after receiving a dose of ethanol for 30 minutes [46].

3.6.1 Dose Calculation

Cisplatin dose according to body weight (e.g. 30 gram mice)

3.6.2 Cisplatin Dose Calculation

Dose administered to mice: 10mg/kg

For a 30g mice:

Required cisplatin dose = (30g × 10g) / 1000g = 0.3mg

each mice received cisplatin dose according to body weight.

3.6.3 Dose Calculation

Requireddose: 10mg/kg

For a 6 mice:

Dose = 0.3 x 6 = 1.8 mg

Drug concentmiceion: 3.6 ml

Per mice 600 microlitre/30g

Silymarine dose according to body weight (e.g 30 gram mice)

Required dose: 50 mg/kg

For a 30g mice: Dose = (50mg × 30g) / 1000g = 1.5 mg

For 6 mice = 1.5 x 6 = 9mg

Volume required = 1.5 mg / 5 mg/ml = 0.3 ml

Mecobalamin 1.5 mg/kg Dose Calculation. Required Dose (mg) = Body weight (g) × Dose (mg/kg) / 1000

2. Volume Required (mL) = Required Dose (mg) / Stock Concentration (mg/m)

Mecobalamin 1.5 mg/kg (Body weight = 30 g)

Dose = 1.5 mg/kg

Required Dose = 30×1.5/1000 = 0.045

Step 2: Volume Required = 0.045/0.15 = 0.3 mL

Mecobalamin 2.5 mg/kg (Body weight = 30 g)

Body weight = 30 g

Dose = 2.5 mg/kg

3.6.4 Step 1: Calculate Required Dose

Required Dose = 30 × 2.5/1000 = 0.075mg

3.6.5 Step 2: Volume Required

Volume Required = 0.075/0.25 = 0.3 mL

FIGURE 3.3: This figure shows the removing the animals from their cage and placing them in clean beaker tare the wait and then placing them on a measuring scale.

TABLE 3.1: Group 1: Control Treatment: Control group: mice received normal saline intraperitoneally (i.p)

Day	**Drug Administered**	**observations**
Day 1	Normal saline (i.p.)	Monitored behavior, recorded body weight
Day 2	Normal saline (i.p.)	Monitored behavior, recorded body weight
Day 3	Normal saline (i.p.)	Monitored behavior, recorded body weight
Day 4	Normal saline (i.p.)	Monitored behavior, recorded body weight

continued on next page

Table 3.1 continued from previous page

Day	Drug Administered	observations
Day 5	Normal saline (i.p.)	Monitored behavior, recorded body weight
Day 6	Normal saline (i.p.)	Monitored behavior, recorded body weight
Day 7	Normal saline (i.p.)	Monitored behavior, recorded body weight
Day 8	Normal saline (i.p.)	Monitored behavior, recorded body weight
Day 9	Normal saline (i.p.)	Monitored behavior, recorded body weight
Day 10	Normal saline (i.p.)	Monitored behavior, recorded body weight

After 24 hours to 10 days of dosing loss in body weight was recorded, restlessness, irritability was noticed.

Table 3.2: Group 2: Cisplatin 10 mg/KG i.p in experimental group

Day	Drug Administered	observations
Day 1	(10mg/kg i.p single dose)	Monitored behavior, recorded body weight
Day 2		Monitored behavior, recorded body weight
Day 3	_	Monitored behavior, recorded body weight
Day 4	_	Monitored behavior, recorded body weight
Day 5	_	Monitored behavior, recorded body weight
Day 6	_	Monitored behavior, recorded body weight
Day 7	_	Monitored behavior, recorded body weight
Day 8	_	Monitored behavior, recorded body weight
Day 9	_	Monitored behavior, recorded body weight
Day 10	_	Monitored behavior, recorded body weight

After 24 hours to 10 days of dosing loss in body weight was recorded, restlessness, irritability was noticed.

Table 3.3: Group 3: Cisplatin and silymarin (10mg/kg and 50mg/kg) Cisplatin and silymarin group (10mg/kg i.p and 50mg/kg orally for ten days)

Day	Drugs Administered	observations
Day 1	Cisplatin and silymarin (10mg/kg and 50mg/kg)	Monitored behavior, recorded body weight
Day 2	Silymarin (50mg/kg)	Monitored behavior, recorded body weight
Day 3	Silymarin (50mg/kg)	Monitored behavior, recorded body weight

continued on next page

Table 3.3 continued from previous page

Day	Drugs Administered	observations
Day 4	Silymarin (50mg/kg)	Monitored behavior, recorded body weight
Day 5	Silymarin (50mg/kg)	Monitored behavior, recorded body weight
Day 6	Silymarin (50mg/kg)	Monitored behavior, recorded body weight
Day 7	Silymarin (50mg/kg)	Monitored behavior, recorded body weight
Day 8	Silymarin (50mg/kg)	Monitored behavior, recorded body weight
Day 9	Silymarin (50mg/kg)	Monitored behavior, recorded body weight
Day 10	Silymarin (50mg/kg)	Monitored behavior, recorded body weight

After 24 hours to 10 days of dosing loss in body weight was recorded, restlessness, irritability was noticed.

TABLE 3.4: Cisplatin and Mecobalamin (10mg/kg and 1.5mg/kg) Cisplatin and Mecobalamin group (10mg/kg i.p and 1.5 mg orally per day)

Day	Drugs Administered	observation
Day 1	Cisplatin and Mecobalamin (10mg/kg i.p and 1.5mg/kg per day)	Monitored behavior, recorded body weight
Day 2	Mecobalamin (1.5mg/kg)	Monitored behavior, recorded body weight
Day 3	Mecobalamin (1.5mg/kg)	Monitored behavior, recorded body weight
Day 4	Mecobalamin (1.5mg/kg)	Monitored behavior, recorded body weight
Day 5	Mecobalamin (1.5mg/kg)	Monitored behavior, recorded body weight
Day 6	Mecobalamin (1.5mg/kg)	Monitored behavior, recorded body weight
Day 7	Mecobalamin (1.5mg/kg)	Monitored behavior, recorded body weight
Day 8	Mecobalamin (1.5mg/kg)	Monitored behavior, recorded body weight
Day 9	Mecobalamin (1.5mg/kg)	Monitored behavior, recorded body weight
Day 10	Mecobalamin (1.5mg/kg)	Monitored behavior, recorded body weight

After 24 hours to 10 days of dosing loss in body weight was recorded, restlessness, irritability was noticed.

TABLE 3.5: Group 5: Cisplatin and Mecobalamin (10mg/kg and 2.5mg/kg per day) Cisplatin and Mecobalamin group (10mg/kg i.p and 2.5mg/kg oral per day)

Day	**Drugs Administered**	**observation**
Day 1	Cisplatin and Mecobalamin group (10mg/kg i.p and 2.5mg/kg per day)	Monitored behavior, recorded body weight
Day 2	Mecobalamin group (2.5mg/kg per day)	Monitored behavior, recorded body weight
Day 3	Mecobalamin group (2.5mg/kg per day)	Monitored behavior, recorded body weight
Day 4	Mecobalamin group (2.5mg/kg per day)	Monitored behavior, recorded body weight
Day 5	Mecobalamin group (2.5mg/kg per day)	Monitored behavior, recorded body weight
Day 6	Mecobalamin group (2.5mg/kg per day)	Monitored behavior, recorded body weight
Day 7	Mecobalamin group (2.5mg/kg per day)	Monitored behavior, recorded body weight
Day 8	Mecobalamin group (2.5mg/kg per day)	Monitored behavior, recorded body weight
Day 9	Mecobalamin group (2.5mg/kg per day)	Monitored behavior, recorded body weight
Day 10	Mecobalamin group (2.5mg/kg per day)	Monitored behavior, recorded body weight

After 24 hours to 10 days of dosing loss in body weight was recorded, restlessness, irritability was noticed.

Dosing for consecutive ten days, mice were sacrificed on 3rd, 7th and 10th day after dosing for blood and tissue collection.

Personal Protective Equipment (PPE) and Hygiene.

Ensured appropriate PPE was utilized so that technician was appropriately protected from accidental blood and/or body fluid exposure,

1. Gloves
2. Eye protection
3. Mask Other PPE indicated in protocol/facility

Hands washed. Gloves changed between animals. Used sharps promptly placed in provided leak-proof, puncture resistant sharps contain.

3.7 Methods of Euthanasia

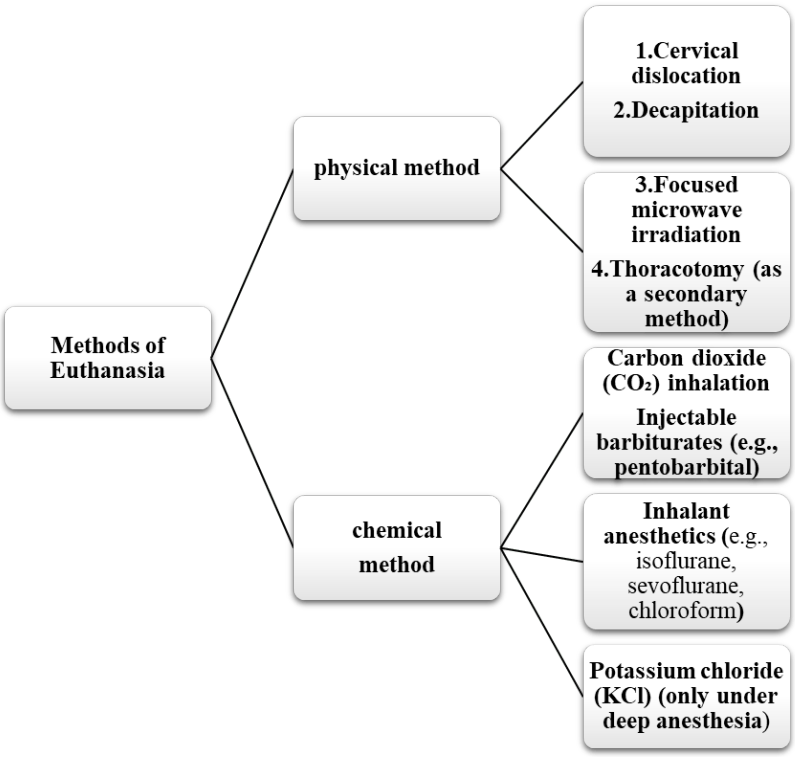

FIGURE 3.4: Methods of euthanasia

Euthanasia means an easy death, an act of humane killing with the minimum of pain, fear and distress.[47].

The chosen procedure should:

1. Cause no pain.

2. Induce rapid loss of consciousness followed by death.
3. Simultaneously interrupt consciousness and reflexes.
4. Require minimal restraint.
5. Minimize excitement and cause minimal distress to the animals.
6. Be suitable for the animal's specific developmental stage.
7. Produce reliable and consistent effects.
8. Allow for safe and straightforward administration by adequately trained staff.
9. Cause minimal psychological or emotional distress to both the animals and the personnel involved.
10. Avoid causing any tissue changes that might interfere with subsequent post-mortem analyses.

Methods of euthanasia fall into categories physical method and chemical method

3.7.1 Physical Methods of Euthanasia in Mice

1. Cervical dislocation
2. Decapitation
3. Focused microwave irradiation
4. Thoracotomy (as a secondary method)

3.7.2 Chemical Methods of Euthanasia in Mice

1. Carbon dioxide (CO_2) inhalation
2. Injectable barbiturates (e.g., pentobarbital)

3. Inhalant anesthetics (e.g., isoflurane, sevoflurane, chloroform)

4. Potassium chloride (KCl) (only under deep anesthesia)

3.7.3 Chemical Methods Inhalant Agents for Mice Euthanasia

Euthanasia via inhaled gases was delayed by the need for the gas to build up to effective concentrations within the tissues. Implementing this method required both a gas-tight chamber and careful safety procedures to mitigate the risk of toxic exposure to personnel.

3.7.3.1 Inhalant agents

The colorless liquid chloroform was highly volatile and poorly soluble in water. It smells nice and non-irritating. Chloroform has a molecular weight of 119.38 g/mol and the chemical formula $CHCl_3$. Chloroform is a chemical that is frequently used in industrial processes and biological laboratories. Animals have been sacrificed under chloroform sedation with seemingly no negative consequences. The animals were placed in a desiccator with the appropriate chemical. To guarantee circulation, the chemical was soaked in cotton wool and put in the desiccator for two minutes before exposure.

3.8 Blood Withdrawal Techniques

3.8.1 Retrobulbar Plexus/Sinus Puncture (Mice – Eye)

Mice were anesthetized using isoflurane in an induction chamber at 3–4% and maintained at 1–2% via nose cone. The animal was placed in a prone position with the head stabilized. A heparinized capillary tube was gently inserted into the medial canthus of the eye at a 30–45° angle toward the rear of the orbit to puncture the retrobulbar venous sinus. Blood was allowed to flow into the tube via capillary action. Upon collection (up to 0.2 mL), the tube was withdrawn and gentle pressure was applied using sterile gauze to prevent

hematoma formation. Animals were monitored post-procedure for signs of ocular damage or distress [48].

3.8.2 Tail Vein Puncture (Mice – Tail)

Got the following supplies ready: a 28 G 1/2 insulin syringe (30 U or 50 U), sterile gauze, gloves, alcohol wipes, a microcapillary blood collection EDTA tube (purple cap), and a plastic restraining holder. Quickly placed the mice in a plastic restraining cone after removing them from their cage. Enclosed the base of the tail with the large end of the cone. Throughout the entire process, make sure the animal was at ease and that its breathing is unhindered. To dilate the vein, immerse the tail in warm water (37 ^{o}C) for approximately one minute. Used a paper towel to pat dry the tail. With the tail was resting on a heating pad, placed the animal face down in its restrainer. To avoid the tail twisting, rotated the entire animal to either side and choose the right or left tail vein (blue line) for sampling. Because the vessels become more superficial in that area, puncture the blood vessels in the terminal third of the tail. The two veins were lateral, and the artery was ventral. Used 70% ethanol wipes to clean the puncture site on the tail. To form an angle in the tail's terminal third, position the tail on the heating pad's edge. This made more room for the sample to be taken and brings the vein to the surface [49].

3.8.3 Sublingual Vein Puncture (Mice – Tongue)

Under isoflurane anesthesia, the animal was placed in dorsal recumbency. The tongue was gently exteriorized using blunt forceps. A small-gauge needle (e.g., 26G) was used to puncture the prominent sublingual vein. Blood droplets were collected directly into micro tubes or capillaries. Homeostasis was achieved with gentle gauze pressure. This method provided rapid, volume blood collection (up to 0.5 mL) with minimal stress when properly performed.

3.8.3.1 Facial Vein Puncture (Mice – Cheek)

Mice were gently restrained manually or using a restraining device. A 21–23G needle or lancet was used to puncture the facial (submandibular) vein located between the eye and base of the jaw. Blood droplets were collected into appropriate tubes without anti-coagulant contamination. Homeostasis was maintained with sterile gauze. This method allowed for repeat sampling and yielded up to 0.2 mL of blood with minimal training.

3.8.4 Isoflurane Anesthesia Control (Mice)

Anesthesia was induced in an induction chamber using 3–4% isoflurane in oxygen and maintained at 1–2% via nose cone. Animals were observed for loss of righting reflex and pedal withdrawal reflex to confirm adequate anesthesia before invasive procedures. Isoflurane was delivered using a precision vaporizer with flow of 1 L/min oxygen. Animals were monitored continuously for respiratory mice, reflexes, and skin color to ensure safe anesthesia levels.

3.8.5 Cardiac Puncture

For terminal blood collection, the animals were deep anesthetized either with chloroform or isoflurane or a combination of ketamine (80-100 mg/kg) and xylazine (10 mg/kg) via intraperitoneal administration. Once unresponsive, the animal was placed in dorsal recumbency. A 1 mL syringe with a 23G needle was placed into the thoracic cavity between the 3rd and 5th intercostal space, directed toward the heart, and blood was slowly aspired from the left ventricle. The animal was euthanized by exsanguinations or through an approved alternate method immediately after the procedure. We used cardiac puncture for blood collection.

3.8.5.1 Material Required

1. General anesthetic agent (chlorofrom) inhaled to effect, usually approximately 3%

2. Syringes (1cc tuberculin or 3cc) c. Needles (23 to 27 gauge; %-1 inch)

3. Gloves.

3.8.5.2 Procedure

1. Before beginning sample collection procedures, deeply anesthetized the mice using the chloroform anesthetic agent.

2. After the animal had achieved the proper level of anesthesia, place it in dorsal recumbency.

3. With the syringe parallel to the mice's midline, attached a needle of the proper size to it and insert it through the diaphragm, bevel up, at a 30–40° angle.

4. Pointed the needle toward the animal's head, just left of and beneath the sternum. It is possible to tilt the needle slightly in the direction of the left shoulder.

5. To created a vacuum inside the syringe, slightly retract the plunger. Then, slowly advance the needle until a blood flash appears in the needle hub.

6. Immobilized the needle and kept aspirating until enough blood was drawn.

3.9 Euthanize the Animal Immediately upon Completion of Blood Collection

1. Cervical dislocation

2. Thoracotomy on both sides.

There are two ways to obtain blood from a cardiac puncture.

1. Left lateral approach

2. An open strategy

A. Lateral left approach

1. Position the animal in lateral recumbency on its right side.
2. Felt the heart on the left lateral thoracic wall between the fifth and sixth ribs, roughly where the elbows were flexed.
3. Slowly inserted the needle perpendicular to the body.

B. Open approach

1. Positioned the animal in a dorsal recumbent position.
2. 70% alcohol on wet skin.
3. About 1 cm caudal to the last rib, make a V-shaped cut through the abdominal wall and skin.
4. Set aside the organs of the abdomen.

Blood in tubes and send for analysis in laboratory.

3.9.1 Extraction of Kidney

After blood collection, mice were sacrificed.

1. Using 11.5 cm surgical scissors, an incision was made through the cutis and fascia to perform a midline laparotomy approximately 2 cm in length in the abdominal region.
2. The scissors were then used as a spreader to separate the connective tissue covering the peritoneum.
3. To access the peritoneal cavity, the peritoneum was incised along the linea alba.

4. To enlarge the cavity, a holding suture was placed into the sternum, with the suture filament lifted and secured over the Fluovac mask.

5. A Colibri retractor was inserted into the peritoneal cavity to expand the opening. The kidney was elevated, carefully dissected, and separated from the surrounding tissues.

6. After rinsing the peritoneal cavity with 0.9% NaCl solution, the abdominal organs were repositioned to their normal anatomical locations.

7. The excised kidney was also washed with 0.9% NaCl solution.

8. Kidney tissues were fixed in 10% phosphate-buffered formalin (pH 7.4) and stored at -40^{o}C for further analysis [50].

3.10 Assay of Glutathione Reductase Activity

3.10.1 Methodology

Glutathione reductase (GSR) activity was determined with follow Carlberg and Mannervik (1975) methodology for measuring antioxidant enzyme activities [51]. The standard marker for enzyme activity was the rate of GSSG oxidation of NADPH at 30^{o}C. The 1 ml reaction system comprised 1.0 mM GSSG, 0.1 mM NADPH, 0.5 mM EDTA, 0.10 M sodium phosphate buffer (pH 7.6), and sufficient glutathione reductase sample to produce an absorbance change of 0.05 to 0.30/min. Under these conditions the glutathione reductase was measured as the oxidation of 1 μmol NADPH/min. The specific activity was calculated in units per mg protein.

The level of reduced glutathione was analyzed according to protocol in the given reference [51].

3.10.2 Reagent Preparation

Three working solutions were prepared in stock buffer (125 mM Na-phosphate, 6.3 mM Na-EDTA, pH 7.5):

a) (I) 6 mM DTNB (Note: May precipitate; gently warm to redissolve before use).

b) (II) 0.3 mM NADPH.

c) (III) ∼50 units/ml Glutathione Reductase (GR).

d) *Stability:* All solutions remain stable for ≥2 weeks at 0^oC.

3.10.3 Assay Setup

a) Combine in a 1-cm pathlength cuvette:

   a) 700 μl Solution I (DTNB)

   b) 100 μl Solution II (NADPH)

   c) Glutathione sample or water (to final volume 1.0 ml)

b) Equilibrate the mixture to 30^oC.

3.10.4 Reaction Initiation & Measurement

a) Initiate the reaction by adding 1 μl of Solution III (GR).

b) Continuously monitor the increase in absorbance at 412 nm (A_{412}) until it exceeds 2.0.

c) *Linearity:* The DTNB reduction rate is linear for samples containing >∼0.5 nmol glutathione. For lower concentrations, calculate the rate using the linear portion of the curve (typically between A_{412} 1.0 and 2.0).

3.10.5 Quantification

a) Determine glutathione content by comparing the observed reaction rate to a standard curve generated with known glutathione concentrations.

b) *Note:* Identical standard curves are obtained for both GSH and GSSG when expressed as GSH equivalents, consistent with prior reports.

3.10.6 Method Modification

a) This protocol differs from the original by employing continuous kinetic monitoring instead of a single endpoint measurement, an adaptation also used by other researchers.

3.10.7 GSH Derivatization (for GSSG-specific measurement)

a) Add 2 μl of neat 2-vinylpyridine per 100 μl of sample solution (pH $>$ 5.5).

b) Mix vigorously for $\sim$1 minute.

c) Incubate at 25^{o}C for 20–60 minutes (time depends on final pH) to ensure complete GSH derivatization.

d) *Note:* 2-Vinylpyridine has low aqueous solubility. Undissolved globules adhering to the vessel walls are normal; they maintain reagent saturation and do not interfere with subsequent steps. The method effectively derivatizes GSH concentrations $\leq$15 mM.

3.10.8 pH Requirement

The reaction between GSH and 2-vinylpyridine requires near-neutral conditions (pH $>$ 5.5) and will not proceed significantly in acidic solutions without prior partial neutralization.

3.10.9 Sample Preparation (Picric Acid Homogenates)

a) Homogenize tissue in 5 volumes of 1% picric acid.

b) Centrifuge to obtain a protein-free supernatant.

c) Direct Derivatization: Add 2 μl of neat 2-vinylpyridine per 100 μl of supernatant. The addition itself may sufficiently raise the pH to 7.0–7.5, enabling the reaction.

3.10.10 Neutralization for Other Precipitants (e.g., Sulfosalicylic Acid)

a) When using protein precipitants like 5-sulfosalicylic acid, explicit base addition is required to reach pH > 5.5.

b) Recommended Base: Triethanolamine is highly effective due to:

   a) Excellent solubility.

   b) pK_a $\sim$7.8, allowing precise control to pH 7.0–7.5 without excessive alkalinity that promotes auto-oxidation.

   c) (Other bases can be used, but triethanolamine offers key advantages).

3.10.11 Mouse Plasma Processing Example (Critical Timing)

a) Blood Collection: Decapitate unanesthetized mice. Collect blood from the neck into a beaker containing 25 μl of 500 mM EDTA (final concentration $\sim$13 mM).

b) Plasma & Deproteinization: Isolate plasma. Within 4 minutes of blood draw, add 0.5 volume of 10% (w/v) 5-sulfosalicylic acid. Mix well.

c) Centrifugation: Centrifuge the acidified plasma. Retain the supernatant.

d) Aliquot & Add Reagent: Transfer 100 μl aliquots of supernatant into plastic vials. Add 2 μl of neat 2-vinylpyridine to each vial.

e) Neutralization: Add 6 μl (45 μmol) of neat triethanolamine to the inside wall of the vial above the liquid level. Cap and mix vigorously until the final pH is 7.0–7.5. This technique minimizes local high base concentrations, reducing auto-oxidation.

f) Derivatization: Incubate vials at 25^{o}C.

g) Stability Assessment: Measure residual glutathione content (GSSG) at 0, 20, and 40 minutes of incubation.

3.10.12 Assay Interference Note

Triethanolamine causes slight interference ($\sim$ 10%) in the glutathione assay. Therefore, standards must contain equivalent concentrations of triethanolamine as present in the samples$\sim$[51].

3.11 Supernant Collection

Kidney specimens were washed then soaked in ice-cold phosphate buffer saline (PBS) 7.4 total volume was 250 ml and were homogenized on ice with a homogenizer (D160, china). To remove cell residue, centrifugation was performed at 8500 rpm for 30 minutes at 24 ^{o}C. In order to prepare supernant collection the PBS buffer was 0.1 % tween 80 PBS buffer 7.4 [52].

Preparation of PBS buffer 7.4

3.11.1 Reagents Required

a) NaCl (Sodium chloride) – 8.0 g

b) KCl (Potassium chloride) – 0.2 g

c) Na_2HPO_4 (Disodium phosphate, anhydrous) – 1.44 g

d) KH_2PO_4 (Monopotassium phosphate) – 0.24 g

e) Distilled water (dH_2O) – up to 1 liter

f) pH meter

g) 1N HCl or NaOH (for pH adjustment if needed)

3.11.2 Procedure

1. Added all the dry reagents (NaCl, KCl, Na_2HPO_4, and KH_2PO_4) into ∼800 mL of distilled water in a beaker.
2. Stirred using a magnetic stirrer until fully dissolved.
3. Measured pH using a calibrated pH meter. 1N NaOH was used to raise the pH to 7.4.
4. Added distilled water to bring the final volume up to 1 liter.
5. Labeled the solution with its name.

3.11.3 Preparation of 0.1% Tween 80 PBS Buffer 7.4.

3.11.3.1 Materials

a) Tween 80

b) 1X PBS (Phosphate Buffered Saline), pH 7.4

c) Measuring cylinder

d) Pipette

e) Stirring rod or magnetic stirrer

f) Beaker or storage bottle

3.11.4 Preparation for 100 mL of 0.1% Tween 80 in PBS

1. Added 0.1 mL (100$\sim\mu$L) of Tween 80 to the PBS.
2. Mixed thoroughly until the Tween 80 was completely dissolved.
3. Used a magnetic stirrer or shook well if using a bottle.
4. Labeled the solution.
5. Stored at room temperature or at 4°C.

3.12 BCA Protein Assay Protocol

For quantifying total protein concentration in a sample, Bicinchoninic Acid assay is a widely used colorimetric method [53].

3.12.1 Purpose:

To determined the protein concentration in liver tissue supernatant using the Bicinchoninic Acid (BCA) assay.

3.12.2 Materials Required:

1. Supernatant from liver tissue
2. Append-draft tube
3. Homogenizer
4. High-speed microcentrifuge
5. Pipette
6. BCA Protein Assay Kit (Reagent A and Reagent B)

7. BSA Standard (2 mg/mL stock)
8. 96-well microplate
9. Micropipettes and sterile tips
10. Distilled water
11. Plate reader

3.12.3 Kidney Tissue Collection and Preparation

Collected sample kidney tissue and immediately placed in a pre-labeled, pre-weighed append-draft tube. Recorded the weight of the tissue. Based on the tissue weight, add volume of 0.1% Tween 80 in PBS buffer 7.4. All tissue had weight between 50mg-100mg. According to weight of tissue 0.1% Tween 80 in PBS buffer 7.4 was added.

E.g. if tissue weight was 50mg then 166.67μL PBS was added. By using this 0.1% Tween 80 in PBS buffer 7.4 was added in all samples [54].

3.12.4 Tissue Homogenization and Centrifugation

Homogenized the tissue thoroughly using a homogenizer. Centrifuged the homogenate at 8500 rpm for 30 minutes at 24^{o}C to remove tissue debris. Supernant was collected.

3.12.5 Preparation of Standards

In 96-well plate standard serial dilutions from BSA stock (2mg/mL) was prepared. Use 20 μL of each dilution per well for the standard curve. Serial dilution (20μL, 15μL,10μL,7.5μL ,5μL, 2.5μL, 0.00). To make 20μL per well, distill water was added.

3.12.6 Sample Preparation

Sample supernant was taken for the sample preparation with 1:10. Mix 1 part sample with 9 parts distilled water (1:10 dilution).

3.12.7 Preparation of Working Reagent (WR)

Reagent A and Reagent B was working reagent and were used as 50:1. If Reagent A 50μL then Reagent B will 1μL. Freshly prepared before used. Add 200 μL of the working reagent (WR) to each well. Gently tapped the plate to mixed for 30 seconds.

3.12.8 Incubation

After adding the working reagent (WR) to samples and standards, incubated the plate at 37^{o}C for 30 minutes. Following incubation, plate was cool to room temperature (approximately 5–10 minutes) before proceeding.

3.12.9 Plate reader

Measured absorbance at 562nm using a plate reader. Note the absorbance calculate the concentration of sample. Constructed the Standard curve and calculated sample protein concentrations based on absorbance values [54].

3.13 ELISA Test

ELISA tests were carried out to define the amounts of tnf-alpha. Each microplate was pre-coated with a specific antibody. Manufacture provided protocol was followed.

3.13.1 ELISA Assay Procedure

3.13.1.1 Prepare Standard Curve (Serial Dilution):

Designate 10 wells on the pre-coated plate for standards. Add 100 μl of Standard Stock Solution (480 ng/L) to wells #1 and #2. Add 50 μl of Standard Dilution Buffer to wells #1 and #2. Mix thoroughly. Transfer 100 μl from wells #1 and #2 to wells #3 and #4. Add 50 μl of Standard Dilution Buffer to wells #3 and #4. Mix thoroughly. *(Concentration: ∼320 ng/L)*. Transfer 50 μl from wells #3 and #4 to wells #5 and #6. Add 50 μl of Standard Dilution Buffer to wells #5 and #6. Mix thoroughly. *(Concentration: ∼160 ng/L)* Transfer 50 μl from wells #5 and #6 to wells #7 and #8. Add 50 μl of Standard Dilution Buffer to wells #7 and #8. Mix thoroughly. *(Concentration: ∼80 ng/L)*. Transfer 50 μl from wells #7 and #8 to wells #9 and #10. Add 50 μl of Standard Dilution Buffer to wells #9 and #10. Mix thoroughly. *(Concentration: ∼40 ng/L)*. Discard 50 μl from wells #9 and #10. Final Standard Concentrations: Well 1/2: 480 ng/L, Well 3/4: 320 ng/L, Well 5/6: 160 ng/L, Well 7/8: 80 ng/L, Well 9/10: 40 ng/L.

Samples and blanks were prepared by first adding 40 μl of Sample Dilution Buffer to each designated sample well, followed by 10 μl of the test sample, ensuring gentle mixing without touching the well walls to achieve a final sample dilution of 1:5. The blank wells were left empty, with no addition of sample or HRP-conjugate reagent in subsequent steps. The plate was then sealed securely with adhesive film and incubated at 37^{o}C for 30 minutes.

During the incubation, the wash buffer was prepared by diluting the concentrated Wash Solution at a ratio of 1:30 (or 1:20 according to the kit instructions) with distilled water, mixing thoroughly. After incubation, the adhesive film was removed, and the liquid contents of all wells were discarded. The plate was firmly blotted dry on clean absorbent paper. Each well was then completely filled with the diluted Wash Buffer and allowed to stand for 30 seconds before discarding. This washing process was repeated a total of five times.

Following washing, 50 μl of HRP-Conjugate Reagent was added to all wells except the blank wells. The plate was resealed with adhesive film and incubated again at 37^{o}C for 30 minutes, followed by another set of five wash cycles as described earlier.

Subsequently, 50 μl of Chromogen Solution A and 50 μl of Chromogen Solution B were added to every well, including blanks, and the plate was gently tapped to mix without forming bubbles. The plate was sealed with adhesive film and incubated at 37^{o}C for exactly 15 minutes in the dark. The reaction was then stopped by adding 50 μl of Stop Solution to each well, with gentle tapping to mix, resulting in a color change from blue to yellow, indicating successful termination of the reaction.

Finally, the absorbance (optical density, OD) of each well was measured at 450 nm within 15 minutes of adding the Stop Solution, using the blank wells to zero the microplate reader. Absorbance values for all standards and samples were recorded, and a standard curve was plotted with absorbance on the y-axis against known standard concentrations on the x-axis. The protein concentrations in the samples were calculated based on their respective absorbance values [55].

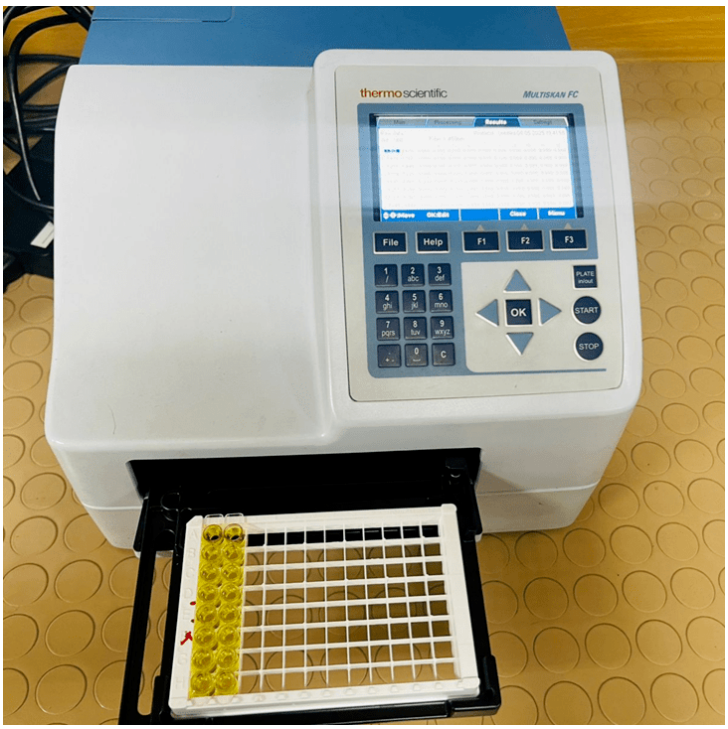

FIGURE 3.5: use of microplate reader to analyze BCA protein assay.

The above figure shows elisa assay based on the colorimetric detection of protein concentration. The protein reduces resulting in the formation to produce a purple complex. The resulting colour can then be measured using microplate reader at 562nm (Photograph taken at faculty of Pharmacy, Capital University of Science and Technology).

3.14 Statistical Analysis

Quantitative data were expresses as mean ± standard deviation (SD). Statistical analysis was performed using Graph Pad Prism 8.0.1 software (GraphPad software USA). One way analysis of variance (ANOVA) followed by post hoc Turkey's multiple comparison test was employed for detection of differences among experimental groups, p-value of $<$ 0.05 was considered a measure of statistical significance. Standard curves were obtained by linear regression and the corresponding concentrations of TNF-α were read off from sample absorbance values for ELISA and BCA assay data. Each experimental group consisted of n=6 animals to ensure sufficient statistical power.

Chapter 4

Results

This chapter presents the experimental findings of the study evaluating the nephroprotective and anti-inflammatory potential of mecobalamin and silymarin in a mouse model of cisplatin induced nephrotoxicity. Glutathione levels determined by performing, Assay of Glutathione Reductase activity and determine NADPH enzyme activity in inflammation [56].

4.1 Study Design

In our study, we developed a mice cisplatin induced kidney toxicity model to evaluate potential recuperative effect of the mecobalamin and silymarin treatment.

Mice were divided into 5 groups:

a) Group-1: mice in Control group received normal saline

b) Group-2: Cisplatin group: mice in this group received cisplatin (10mg/kg i.p single dose)

c) Group-3: Cisplatin and silymarin group (10mg/kg i.p and 50mg/kg orally for ten days)

d) Group-4: Cisplatin and Mecobalamin group (10mg/kg i.p and 1.5 mg orally per day)

e) Group-5: Cisplatin and Mecobalamin group (10mg/kg i.p and 2.5 mg orally per day)

In this study, cisplastin treatment causes a significant ($p < 0.05$) reduction in the renal level antioxidant enzyme ; reduced glutathione (GSH), compared to normal control group, suggesting impaired antioxidant defense mechanisms (Table 4.1).

However Treatment with Mecobalamin 1.5mg and Mecobalamin 2.5mg significantly ($p < 0.05$) improved GSH levels in and renal tissue, as compared to Cisplatin group (Table 01). These results are comparable to the positive control silymarin, also causes significant improvement in the level of GSH in renal tissues as compared to cisplastin group (Table 4.1).

TABLE 4.1: Effects of Cisplatin , Silymarin and Mecobalamin 1.5 mg and 2.5 mg on the reduced glutathione anti-oxidant biomarkers.

Group	**GSH((nmol/mg protein))**
Normal control	46.27 ± 0.24
Cisplatin	15.73 ± 0.25###
Cisplatin+ Silymarine	39.40 ± 0.39***
Cisplatin+ Mecobalmin 1.5 mg	31.01 ±0.16***
Cisplatin+ Mecobalamin 2.5mg	34.04 ± 0.20***

Silymarine and cisplatin were utilized as positive and negative controls, respectively. n = 6, data represent mean ± SEM. Compared to normal control group (### $P < 0.001$), compared to Cisplastin -induced group (**$P < 0.01$, ***$P < 0.001$).

4.2 Inflammatory Marker Analysis

Inflammatory biomarker levels were quantified using an ELISA-based method, and group-wise to estimate biomarker concentrations with reference to a standard curve. The results

discussed with respect to the dose-dependent effects of the test compounds and their mechanistic relevance in mitigating cisplatin induced renal injury [56].

After collecting blood via cardiac puncture, the mice were sacrificed, and their kidneys were excised. The kidney tissues were then stored in phosphate-buffered saline (PBS, pH 7.4) for biochemical analysis. First BCA analysis was performed for measure concentration of inflammatory marker TNF-α, and then Elisa was performed for quantification of TNF-α.

4.2.1 BCA Protein Assay Protocol

The Bicinchoninic Acid assay is a widely used colorimetric method for quantifying total protein concentration in kidney tissue lysates obtained from experiments.

The BCA assay is based on a colorimetric detection and quantification of total protein by chelation of Cu^{1+} with BCA in alkaline conditions. Absorbance was read at 562 nm and concentrations were determined from a standard curve consisting of known protein concentration. Standard Curve for protein concentration A standard curve of protein concentrations ranging from 0 to 20 μg/μl was generated and the absorbance values at 562 nm were used to create the linear regression equation in order to extrapolate the concentration from unknown samples [57].

TABLE 4.2: Quantification of total protein

Sr no	**0bs.**	**conc.(μg/μl)**
1	0	0
2	0.15	2.5
3	0.201	5
4	0.234	7.5
5	0.468	10
6	0.588	15
7	0.8	20

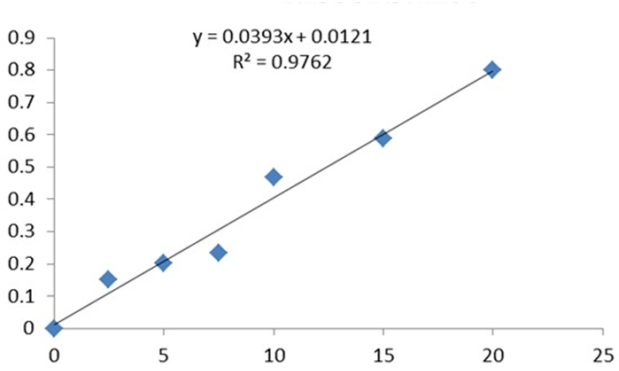

FIGURE 4.1: A standard curve of protein concentration used to create a linear regression equation (BCA)

TABLE 4.3: BCA protein concentration experimental group

Groups	**Dose**	**conc.(μg/μl)**
Normal control group	-	10.60 ± 0.97
Cisplatin group	10mg/kg	20.34 ± 1.48
Silymarin group	50mg/kg	13.08 ± 2.26
Mecobalamin	1.5mg/kg	15.39 ± 1.09
Mecobalamin	2.5mg/kg	12.24 ± 0.58

The inflammation is a critical pathological process of cisplatin induced nephrotoxicity. Pro-inflammatory cytokines including TNF alpha level enhanced in kidney inflammation. Inflammatory markers were assessed in the kidney tissue of all experimental groups.

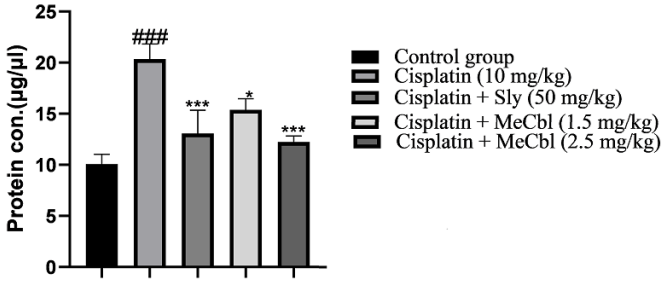

FIGURE 4.2: Effect of standard reference silymarin at 50 mg/kg and mecobalamin at both doses (1.5 mg low dose and 2.5 mg/kg high dose) in cisplatin induced nephrotoxicity injury in mice, as determined by BCA assay. Data were presented as mean ± standard deviation (n=6). Statistical Statistical significance was determined by ANOVA followed by post-hoc analysis.*p<0.05, **p<0.01, ***p<0.001 compared to the cisplatin group.

Cisplatin 10 mg/kg administration caused increase in expression TNF -α in the kidney compared to the intact control group. Mecobalamin 1.5mg/kg administration post administration of cisplatin, down regulated the expression of TNF alpha mecobalamin 1.5mg/kg (low dose) + cisplatin (10mg/kg) group But mecobalamin 2.5 mg/kg (high dose) + cisplatin (10mg/kg) group yield relative better result. Silymarin 50mg/kg+ cisplatin (10mg/kg) group also show reduction in Levels of TNF-α but it has less effect than mecobalamin 2.5mg. Administration of mecobalamin1.5mg/kg, mecobalamin 2.5mg/kg and cisplatin 50mg/kg in three groups caused a significant decrease of the levels of TNF-α compared to the groups that received cisplatin only. This study assesses the anti-inflammatory potential of treatments in suppressing TNF-α levels compared to cisplatin induced expression.

4.2.2 TNF-α Levels

TNF-alpha quantitative measurement of TNF-alpha in kidney tissue was performed using enzyme-linked Immunosorbent assay (ELISA) with standard curves using known concentration standard dilution series of TNF-alpha ranging from 0 to 90 μg/ml. The typical absorbance values of the standards were very straight linear, 2.532 at 90μg/ml, 1.721 at 60μg/ml 0.981 at 30μg/ml. 0.7011 at 15 μg/ml, and 0.407 at 7.5 μg/ml to establish assay sensitivity and reliability [58].

4.2.2.1 Evaluation of the Inflammatory Marker TNF-α using ELISA

In mice model of cisplatin induced nephrotoxicity, inflammatory biomarker levels were quantified using an ELISA-based method, and group-wise to estimate biomarker concentrations with reference to a standard curve. The results were discussed with respect to the dose-dependent effects of the test compounds and their mechanistic relevance in mitigating cisplatin induced kidney injury.

Using an ELISA-based method, levels of inflammatory biomarkers TNF-α, estimate in experimental groups relative to a standard concentrations curve.

Standard Curve for Quantification of TNF-α A standard curve was created with TNF-α concentrations of 0μg/μl, 15 μg/μl, 15 μg/μl, 30μg/μl, 60 μg/μl, and 90 μg/μl made from serial dilutions of the TNF-α standard. Absorbance readings were taken at 450 nm and plotted a standard regression equation, which was then used to extrapolate TNF-α concentration in kidney tissue lysate samples.

TABLE 4.4: Standard. TNF-α concentrations

Sr.no	**0bs.**	**conc.(μg/μl)**
1	0.055	0
2	0.407	7.5
3	0.701	15
4	0.981	30
5	1.721	60
6	2.532	90

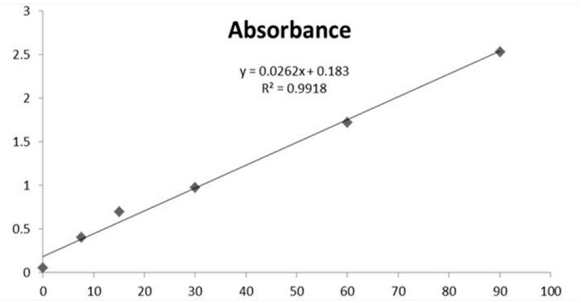

FIGURE 4.3: A standard curve of protein concentration used to create a linear regression equation (TNF-α)

4.2.2.2 TNF-α Levels in Experimental Groups

TNF-α concentration were calculated from the absorbance values for each sample as obtained from the standard curve. Below are the results for all groups.

TABLE 4.5: Elisa test. TNF-α concentration in experimental group

Groups	**Dose**	**conc.(μg/μl)**
Control group	-	3.98 $\pm$ 0.55
Cisplatin group	10mg/kg	7.69 $\pm$ 0.95
Silymarin group	50mg/kg	4.63 $\pm$ 0.35

continued on next page

Table 4.5 continued from previous page

Groups	Dose	conc.(μg/μl)
Mecobalamin group	1.5 mg/kg	5.35 ± 0.20
Mecobalamin group	2.5mg/kg	4.27 ± 0.64

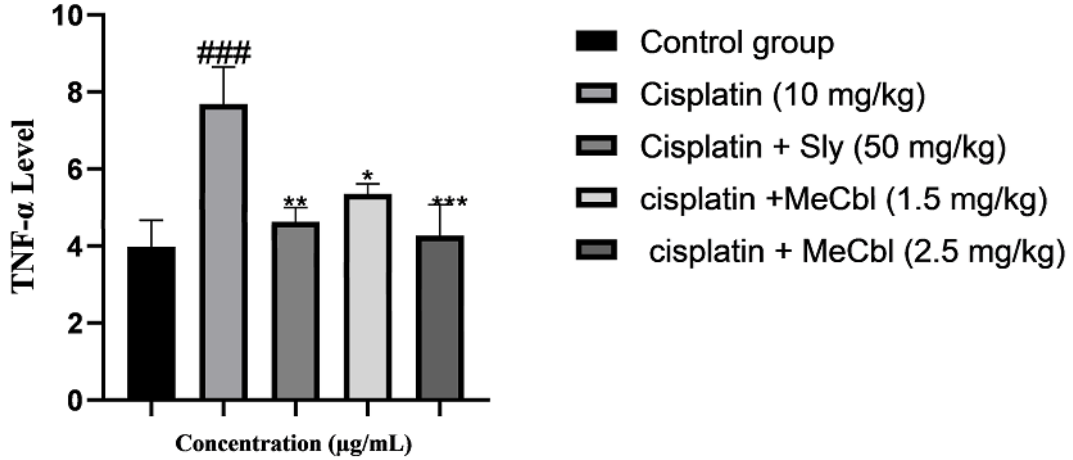

FIGURE 4.4: Effect of Mecobalamin and silymarin on serum tumor necrosis factor-alpha (TNF-α) levels in cisplatin induced renal injury in mice. Data were presented as mean ± standard deviation (n=6). Statistical significance was determined by ANOVA followed by post hoc post-hoc analysis. *p<0.05, **p<0.01, ***p<0.001 compared to the cisplatin group.

TNF-α expression in cisplatin i.p (10mg/kg) resulted in markedly higher as compared to the intact control, indicating significant renal inflammation. The average absorbance values for the cisplatin group were significantly higher than the average absorbance values for the control group confirming cisplatin treatment influences pro-inflammatory cytokine up-regulation. When Mecobalamin 1.5 mg/kg (low dose) was given after cisplatin exposure, TNF-α levels decreased indicating a minor anti-inflammatory effect.

The Mecobalmin2.5 mg/kg (high dose) + cisplatin group showed an even stronger reduction in TNF-α activity suggesting a dose-dependent effect in inhibiting cisplatin induced renal inflammation. The silymarin 50 mg/kg + cisplatin group also exhibited a reduction in TNF-α levels when compared to the cisplatin only group, but the effect was is less than high dose of Mecobalamin . The cisplatin+ mecobalamin 2.5 mg/kg group had the greatest anti-inflammatory effect suggesting that mecobalamin 2.5 mg/kg was the most effective treatments for mediating levels of TNF-α and reducing cytokine-induced renal

injury. Across all treatment groups, a history significantly lower concentrations of TNF-α in the cisplatin + mecobalamin 1.5 mg/kg, cisplatin + mecobalamin 2.5 mg/kg, and cisplatin + silymarin 50 mg/kg treatment groups relative to the cisplatin alone group; therefore, all treatment groups demonstrated clinical utility with these pharmacological agents in reducing cisplatin induced renal inflammation. The results indicate a dose-dependent anti-inflammatory effect with mecobalamin , outperforming the silymarin. The results also confirm Mecobalamin potentially reducing inflammation.

4.3 Histopathological Assessment

NADPH oxidase enzymes will be examined in the kidney tissues.

For the fixation, kidney samples will be kept in a 10% formalin buffer solution. After being dehydrated using increasing alcohol grades (80, 90, and 100%), tissue samples will be embedded in paraffin. A microtome will be used to cut each sample into thin sections (4-5 mm). The sections will be stained using hematoxylin and eosin (H&E) stain. A compound microscope will be used for microphotography. (Nikon-187842, Japan) at 40X [59].

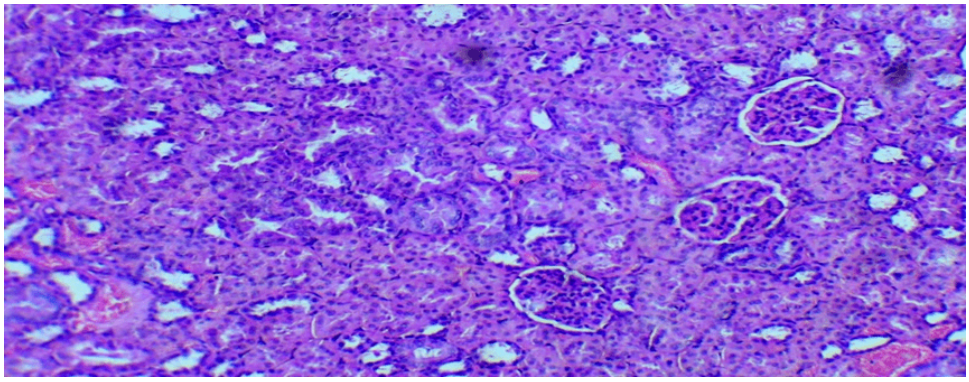

FIGURE 4.5: H&E staining of cross-sectional kidney tissue across experimental. The figure above shows H&E staining of control group at 40x magnification. The study of tissue and cells under a microscope "Control group" shows normal glomerulus , renal corpuscle, bowman's capsule, proximal tubules, and cortex all are intact.

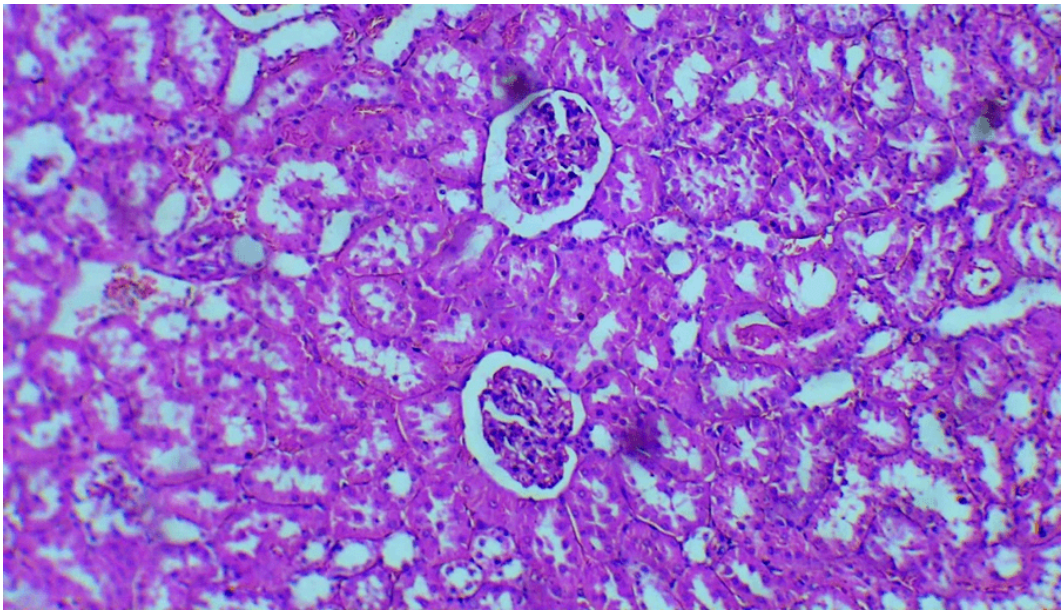

FIGURE 4.6: H&E staining of cross-sectional kidney tissue across experimental. The figure above shows H&E staining of drug group at 40x magnification. The study of tissue and cells under a microscope "Drug group" cisplatin 10mg/kg i.p shows damaged glomerulus, renal corpuscle, bowman's capsule, proximal tubules, and cortex all are not intact. (tissue necrosis ,inflammation , glomerulus integrity is not intact.

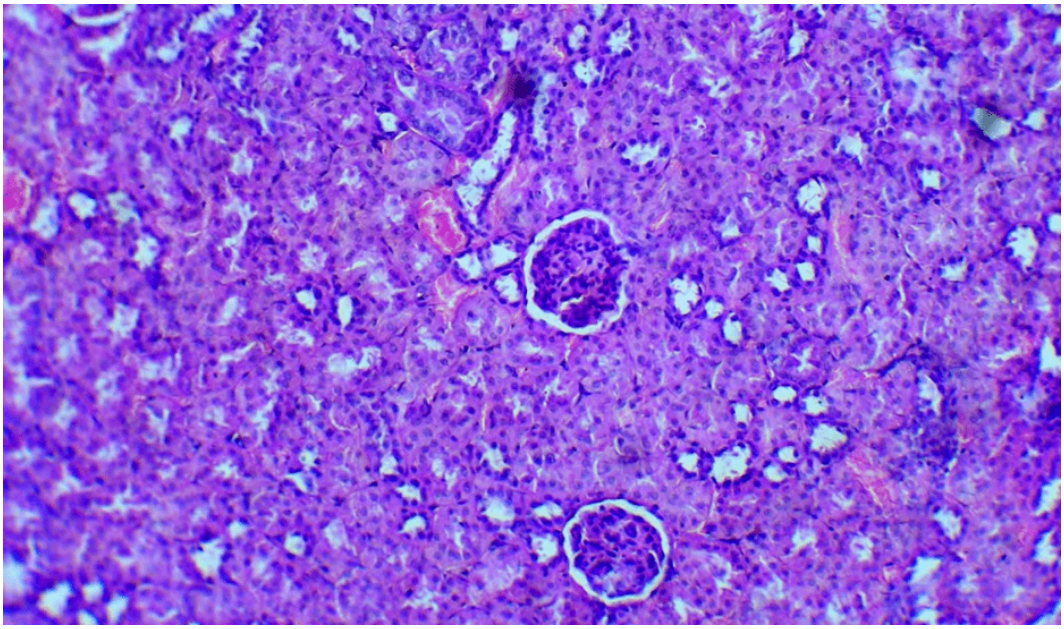

FIGURE 4.7: H&E staining of cross-sectional kidney tissue across experimental. The figure above shows H&E staining of drug group at 40x magnification. The study of tissue and cells under a microscope "Drug group + silymarin " cisplatin 10mg/kg i.p and silymarin 50mg/kg oral shows damaged glomerulus , renal corpuscle, bowman's capsule, proximal tubules, and cortex all are not intact. (tissue necrosis ,inflammation , glomerulus integrity is intact. (recovery seen in tissues)

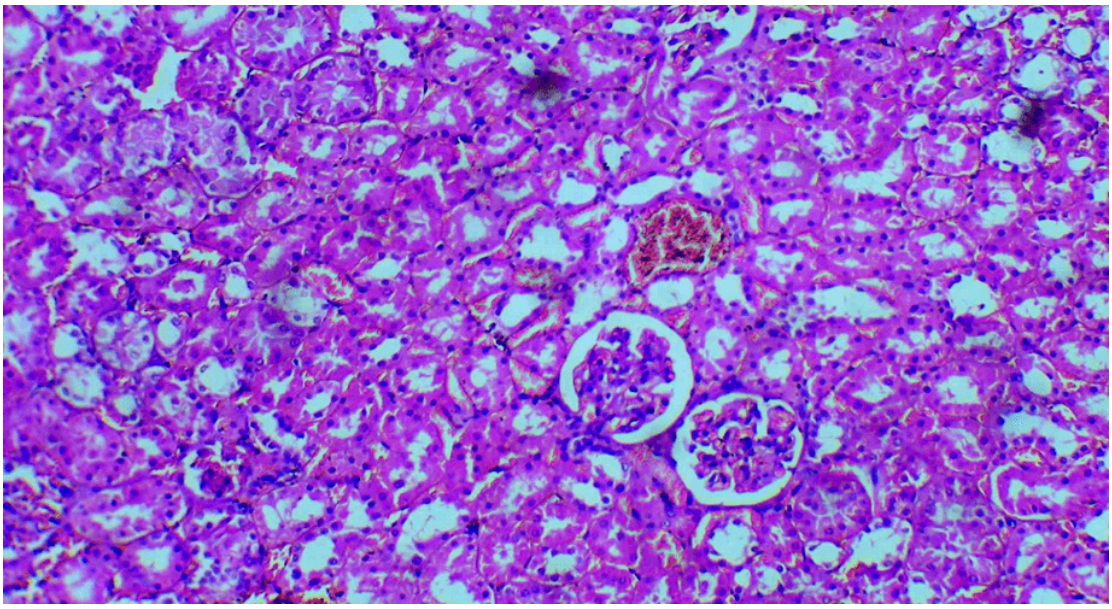

FIGURE 4.8: H&E staining of cross-sectional kidney tissue across experimental. The figure above shows H&E staining of drug group at 40x magnification. The study of tissue and cells under a microscope "Drug group + mecobalamin" cisplatin 10mg/kg i.p and mecobalamin 1.5mg/kg oral shows no damaged glomerulus , renal corpuscle, bowman's capsule, proximal tubules, and cortex all are intact. (recovery seen in tissues)

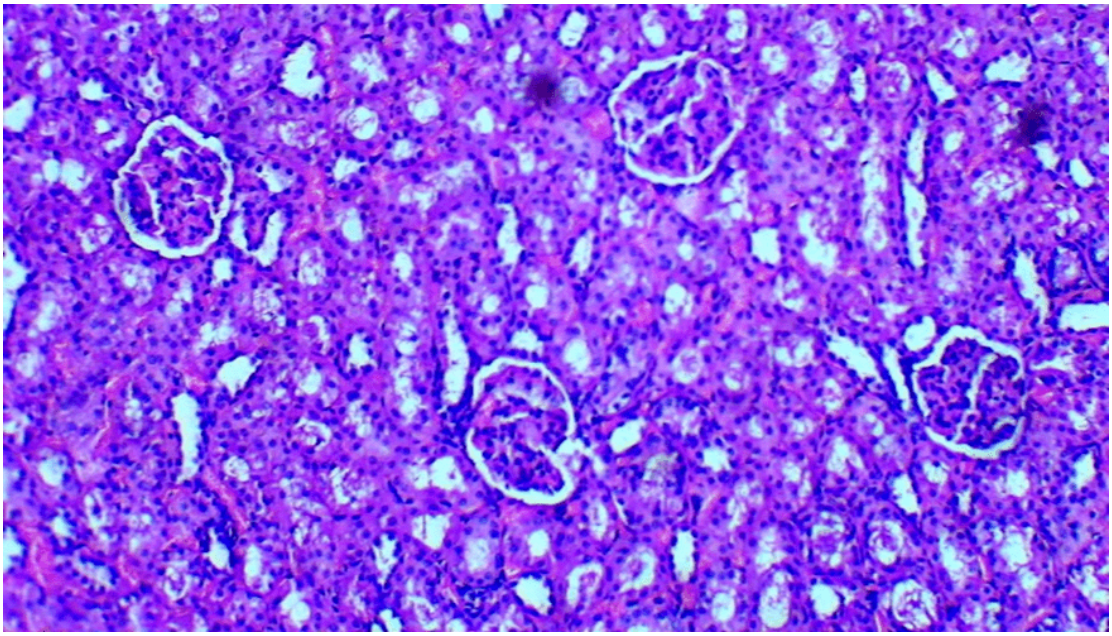

FIGURE 4.9: Hematoxylin and Eosin staining of cross-sectional kidney tissue across experimental. The figure above shows H&E staining of drug group at 40x magnification. The study of tissue and cells under a microscope "Drug group + mecobalamin " cisplatin 10mg/kg i.p and mecobalamin 2.5mg/kg oral shows no damaged glomerulus , renal corpuscle, bowman's capsule, proximal tubules, and cortex all are intact. (significant recovery seen in tissues)

Chapter 5

Discussion

5.1 Cisplatin-Induced Nephrotoxicity

The chemotherapeutic cisplatin is effective against multiple solid tumors (testis, bladder, ovary, lung), but its use is restricted by dose-dependent nephrotoxicity, which can induce acute kidney injury (AKI). Key mechanisms underlying this kidney damage include oxidative stress, mitochondrial dysfunction, inflammation, and apoptosis in renal tubular cells. Renal structure and function significantly deteriorate as a result of these consequences, which were evident in the control group of the current study (cisplatin-only).

The aims of our study was to compare the effectiveness of silymarin, a recognized hepatoprotective and antioxidant agent, with mecobalamin, an bioactive form of vitamin B12 for the purpose of evaluating the possible nephroprotective benefits of mecobalamin. From the biochemical and histological studies, it was shown that mecobalamin significantly reduced cisplatin-induced kidney damage, and especially after being given the maximum dose of 2.5 mg/kg. This study examined the protective effects of mecobalamin against cisplatin nephrotoxicity in mice. Collectively, the results suggest mecobalamin can significantly reduce renal damage induced by cisplatin, especially at the high dose of mecobalamin (2.5 mg/kg), through biochemical endpoints, behavioral outcomes and by acting on cytokines. On the whole, the research has provided the first evidence investigating the nephroprotective effects of mecobalamin, a coenzyme form of vitamin B12,

which is known to counteract cisplatin-directed cellular oxidative stress and inflammation from cisplatin-induced toxicity.

The cisplatin nephrotoxicity mechanisms found in this investigation align with previous discoveries. In renal tissues, cisplatin significantly increased TNF-α levels and depleted glutathione (GSH), suggesting increased oxidative stress and inflammation. Significant histological abnormalities, such as tubular necrosis, loss of brush boundary integrity, and interstitial inflammation, were linked to these metabolic modifications. TNF-α, a crucial pro-inflammatory cytokine, has been extensively linked to cisplatin-induced tubular damage by activating the NF- B pathway and drawing immune cells to the injury site.

There was dose-dependent nephroprotection shown by mecobalamin. When mice were given 2.5 mg/kg of mecobalamin instead of cisplatin alone, their TNF-α levels were much lower, and their GSH levels were recovered. This suggests that mecobalamin may have a function in lowering oxidative damage and inflammation. These results are consistent with earlier research that demonstrated mecobalamin reduces inflammation and improves antioxidants by scavenging reactive oxygen species (ROS), increasing glutathione synthesis, and regulating cytokine production.

Further supporting mecobalamin's cytoprotective effects in renal tissues is the fact that it is known to promote methionine synthesis and methylation processes, which are essential for DNA repair and cellular recovery. Histopathological improvements in the high-dose mecobalamin group, which had less inflammatory infiltration and comparatively maintained renal architecture, further supported the preventive impact of the supplement.

In contrast to Silymarin a common antioxidant used for hepatoprotection, silymarin, was used in this investigation as a comparison therapy. High-dose mecobalamin was more effective than silymarin in reducing inflammatory indicators and histopathological damage, even though silymarin also decreased TNF-α levels and increased GSH content. Silymarin's quick metabolism and poor oral bioavailability may be the cause of this result, as they restrict its systemic efficacy unless used in combination therapy or modified formulations.

Interestingly, prior research on the renoprotective benefits of silymarin in humans has produced conflicting findings. This could be because of dosage restrictions and inter-individual differences in absorption. The water-soluble nature of mecobalamin and its superior intracellular retention, on the other hand, may provide a more reliable therapeutic impact.

5.2 Cisplatin Powerful Chemotherapeutic Agent

Cisplatin is a powerful chemotherapeutic agent employed in numerous malignancies in the modern oncology clinic. The use of cisplatin is associated with nearly 1/3 of individuals treated experience nephrotoxicity of some degree. The nephrotoxic effects of cisplatin are largely attributed to oxidative stress, inflammation, DNA damage, and mitochondrial dysfunction. In this study, the induction of nephrotoxicity by administration of cisplatin (10 mg/kg) caused a measured increase in serum TNF-α levels and impaired glutathione balance which is consistent with the known pathological processes. Histopathological and biochemical changes elicited by cisplatin, including increased pro-inflammatory cytokines, decreased antioxidants, are consistent with earlier documentation, demonstrating that this dose causes adequate acute kidney injury in mice. This model established a strong basis for investigating mecobalamin's possible therapeutic benefits.

5.3 Nephroprotective Role of Mecobalamin

Mecobalamin is a coenzyme form of vitamin B12 that recently has been recognized as providing benefits beyond dealing with the problem of neuropathy. Mecobalamin enhances antioxidant defenses, reduces oxidative stress, and inhibits apoptosis. In this study, the high-dose mecobalamin group (2.5 mg/kg) presented improvements in antioxidant glutathione levels, and a reduction in TNF-α expression compared to the cisplatin-only group, and was even better than the silymarin-treated group. This observations supports the previous reports of the mecobalamin scavenging effects on ROS, and as a valuable

modulator in redox balance in the body. The inhibition of caspase-3 activation and decreasing levels of TNF-α fits the mechanisms for its protective role in models of oxidation and inflammation.

Comparison with Silymarin, a well-known hepatoprotective, antioxidant agent was employed as a standard comparator. While silymarin (50 mg/kg) provided some protection, mecobalamin at 2.5 mg/kg produced dramatically better results in terms of glutathione preservation and TNF-α suppression. Consequently, mecobalamin may represent an alternative single nephroprotective agent or alternative nutrients that could be used with silymarin when silymarin alone does not provide satisfactory and complete protection.

5.4 Dose-Dependent Effects

The study established a clear dose-dependent nephroprotective effect of mecobalamin. Both doses of 1.5 mg/kg and 2.5 mg/kg improved outcomes in comparision to cisplatin alone, however the higher dose provided higher benefit overall in all markers. This suggests that the nephroprotective effect of mecobalamin may reach maximal benefit, dependent on clinical dosing. Mechanistic Insights

Mecobalamin's nephroprotective mechanisms include:

5.4.1 Antioxidant role

Promoting glutathione synthesis and lowering ROS levels. - Anti-inflammatory actions: Inhibiting TNF-α and its subsequent cytokines.

5.4.2 Mitochondrial Protective Ability

Protecting mitochondrial function and inhibiting apoptosis, thereby preventing cell death.

5.4.3 DNA Repair Facilitation

Assisting with DNA synthesis and repair, which is disturbed by cisplatin.

All of these mechanisms work together to protect renal tissue and promote better cellular homeostasis after a toxic event. Clinical Implications Though there are currently no recognized antidotes for nephrotoxicity from cisplatin use, mecobalamin's safety profile, recognized role in antioxidant pathways, and anti-inflammatory pathways, provide much translational potential. Plus, there is oral bioavailability and mostly no side effects (it's cheap!). Mecobalamin could serve as an adjunct therapy to cisplatin-based chemotherapy, demonstrating significant benefits as it relates to renal complications associated with cisplatin.

5.5 Study Limitations

Limitation of this study, Although we have made promising results, there are a number of limitations:

5.5.1 Sample Size

Six mice per group was enough for preliminary evaluation, but validation should be carried out in larger cohorts.

5.5.2 Time

The study period was limited to ten days, which did not allow for an evaluation of the long-term effects of renal recovery or chronic toxicity.

5.5.3 Confirmation by Histology

Biochemical markers were used, but confirming by histopathological examination would validate the interpretation.

5.5.4 Gender Specificity

We only used female mice, possibly limiting generalizability.

Chapter 6

Conclusion and Future Work

The study showed that mecobalamin, specifically 2.5 mg/kg, significantly decreased cisplatin nephrotoxicity in mice. The results demonstrate that mecobalamin's antioxidant and anti-inflammatory properties play a main role in its nephroprotective mechanism. As mecobalamin at 2.5 mg/kg showed a stronger reduction in TNF-α and also caused significant improvement in the level of GSH (34.04 $\pm$ 0.20 nmol/mg protein). The study of tissue and cells under a microscope "Drug group + mecobalamin" cisplatin 10mg/kg i.p and mecobalamin 2.5mg/kg oral also showed no damaged glomerulus , renal corpuscle, bowman's capsule, proximal tubules, and cortex all are intact (significant recovery seen in tissues) and due to its very safe profile, mecobalamin is promising as supportive therapy in patients receiving cisplatin chemotherapy.

6.1 Future Recommendations

The next step in research is to further investigate the findings in order to support their potential clinical relevance. Future studies should expand upon these findings to validate its clinical utility and explore its integration into standard treatment protocols.

Based on the findings and limitations of this study, the following future research directions are recommended:

6.1.1 Expanded Animal Models

Conduct studies using larger animal cohorts, including both male and female mice of different ages, to assess sex- and age-related differences in response to mecobalamin treatment.

6.1.2 Histopathological Correlation

Include histological evaluation of kidney tissues to confirm biochemical changes and provide morphological evidence of renal protection.

6.1.3 Extended Study Duration

Assess long-term renal recovery and the potential for mecobalamin to prevent chronic kidney disease (CKD) following cisplatin exposure.

6.1.4 Mechanistic Studies

Investigate additional molecular pathways involved in mecobalamin's nephroprotective effects, such as mitochondrial dynamics, apoptotic markers (e.g., caspase-3, BAX, Bcl-2), and oxidative stress indicators (e.g., MDA, SOD, catalase).

6.1.5 Comparative Efficacy

Compare mecobalamin with other known nephroprotective agents (e.g., N-acetylcysteine, curcumin, resveratrol) to determine relative potency and potential synergistic effects.

6.1.6 Dose Optimization

Explore a broader range of mecobalamin doses to determine the optimal therapeutic window for nephroprotection without toxicity.

6.1.7 Pharmacokinetics and Safety Profile

Evaluate the pharmacokinetics, tissue distribution, and long-term safety profile of repeated mecobalamin administration.

6.1.8 Clinical Trials in Humans

Design pilot clinical studies to evaluate the safety and efficacy of mecobalamin in cancer patients receiving cisplatin-based chemotherapy.

6.1.9 Tumor Interaction Assessment

Confirm that mecobalamin does not reduce cisplatin's anticancer efficacy by conducting parallel studies in tumor-bearing animal models.

6.1.10 Combination Therapy Studies

Investigate the effectiveness of mecobalamin in combination with hydration therapy, magnesium supplementation, or other nephroprotective strategies currently used in clinical practice.

Bibliography

[1] M. Perše, "Cisplatin mouse models: Treatment, toxicity and translatability," *Biomedicines*, vol. 9, no. 10, p. 1406, Oct 2021.

[2] C.-Y. Fang, T.-J. Yu, Y.-C. Liao, C.-Y. Lin, M.-C. Yu, and M.-C. Chen, "Natural products: Potential treatments for cisplatin-induced nephrotoxicity," *Acta Pharmacologica Sinica*, vol. 42, no. 12, pp. 1951–1969, Dec 2021.

[3] A. Džidić-Krivić, M. Šljivić Husejnović, L. Čiva, M. Hadžić, A. Mujkić, E. Vucić, J. Šutković, and S. Škrbo, "Unveiling drug induced nephrotoxicity using novel biomarkers and cutting-edge preventive strategies," *Chemico-Biological Interactions*, vol. 388, p. 110838, Jan 2024.

[4] V. Gounden, H. Bhatt, and I. Jialal, "Renal function tests," in *StatPearls [Internet]*. Treasure Island (FL): StatPearls Publishing, 2024, available from: https://www.ncbi.nlm.nih.gov/books/NBK507821/.

[5] P. A. Gallardo and C. P. Vio, *Functional anatomy of the kidney*. Cham, Switzerland: Springer, 2022, pp. 7–28.

[6] A. Rizki-Safitri, T. Traitteur, and R. Morizane, "Bioengineered kidney models: methods and functional assessments," *Function*, vol. 2, no. 4, p. zqab026, 2021.

[7] H. Levassort and M. Essig, "The kidney, its anatomy and main functions," *Soins. Gérontologie*, vol. 29, no. 165, pp. 10–20, Jan 2024.

[8] S. Krishnan *et al.*, "Microvascular dysfunction and kidney disease: Challenges and opportunities?" *Microcirculation*, vol. 28, no. 3, p. e12661, 2021.

[9] C. G. Lebedenko and I. A. Banerjee, "Enhancing kidney vasculature in tissue engineering—current trends and approaches: A review," *Biomimetics*, vol. 6, no. 2, p. 40, 2021.

[10] L. Gaydarski, T. Batsalova, I. Dincheva, and B. Dzhambazov, "Unraveling the complex molecular interplay and vascular adaptive changes in hypertension-induced kidney disease," *Biomedicines*, vol. 12, no. 8, p. 1723, Aug 2024.

[11] A. Javed, S. Bashir, M. Imran, M. U. Ijaz, M. Shahzad, and A. Irfan, "Navigating nephropathy and nephrotoxicity: Understanding pathophysiology unveiling clinical manifestations, and exploring treatment approaches," *Journal of Basic and Clinical Physiology and Pharmacology*, vol. 36, no. 2–3, pp. 69–93, Mar 2025.

[12] R. Yadav, N. Bhardwaj, D. Poonia, S. Bhardwaj, A. Kumari, V. Kumar, S. Kumar, and V. Kumar, "Environmental toxicants and nephrotoxicity: Implications on mechanisms and therapeutic strategies," *Toxicology*, p. 153784, Apr 2024.

[13] V. E. Sobolev *et al.*, "Molecular mechanisms of acute organophosphate nephrotoxicity," *International Journal of Molecular Sciences*, vol. 23, no. 16, p. 8855, 2022.

[14] L. J. Appel *et al.*, "Estimated glomerular filtration rate, albuminuria, and adverse outcomes: an individual-participant data meta-analysis," *JAMA*, vol. 330, no. 13, pp. 1266–1277, 2023.

[15] V. Sharma and T. G. Singh, "Drug induced nephrotoxicity-a mechanistic approach," *Molecular Biology Reports*, vol. 50, no. 8, pp. 6975–6986, Aug 2023.

[16] Z.-L. Li *et al.*, "Renal tubular epithelial cells response to injury in acute kidney injury," *EBioMedicine*, vol. 107, p. 104241, 2024.

[17] P. Wang *et al.*, "Roles of dna damage in renal tubular epithelial cells injury," *Frontiers in Physiology*, vol. 14, p. 1162546, 2023.

[18] E. Tasinato, "Development of an in vitro 3d model of the proximal tubule interstitial interface as a high throughput renal fibrosis assay platform," Ph.D. dissertation, School of Medicine, Newcastle University, Newcastle upon Tyne, UK, 2024.

[19] L. E. Thompson, "Cisplatin-induced nephrotoxicity: Risk factors and mitigation strategies," Ph.D. dissertation, Anschutz Medical Campus, University of Colorado Denver, Aurora, CO, USA, 2024.

[20] A. M. Romani, "Cisplatin in cancer treatment," *Biochemical Pharmacology*, vol. 206, p. 115323, Dec 2022.

[21] K. R. McSweeney, L. E. Gerschenson, L. E. Bennett, S. Chaudhuri, A. Dhyani, and S. A. Lewis, "Mechanisms of cisplatin-induced acute kidney injury: Pathological mechanisms, pharmacological interventions, and genetic mitigations," *Cancers*, vol. 13, no. 7, p. 1572, Apr 2021.

[22] J. Du, "Models and mechanisms of chemotherapy-induced side effects," Ph.D. dissertation, Department of Medicine, Washington University, St. Louis, MO, USA, 2025.

[23] C. A. Oliveira, G. H. Pavan, B. Castaldi, F. T. Borges, N. O. S. Câmara, C. K. Fujihara, and R. Zatz, "An integrated view of cisplatin-induced nephrotoxicity, hepatotoxicity, and cardiotoxicity: Characteristics, common molecular mechanisms, and current clinical management," *Clinical and Experimental Nephrology*, vol. 28, no. 8, pp. 711–727, Aug 2024.

[24] M. H. Fawzy *et al.*, "Molecular mechanisms of cisplatin induced nephrotoxicity," *Records of Pharmaceutical and Biomedical Sciences*, vol. 6, no. 3, pp. 128–135, 2022.

[25] E. V. Potapova, M. V. Yakovleva, A. V. Kazantsev, A. A. Artyukhov, V. G. Zgoda, V. V. Pleshkan, and E. D. Sverdlov, "Detection of nadh and nadph levels in vivo identifies shift of glucose metabolism in cancer to energy production," *The FEBS Journal*, vol. 291, no. 12, pp. 2674–2682, Jun 2024.

[26] A. S. Abdullah *et al.*, "Green synthesis of silymarin–chitosan nanoparticles as a new nano formulation with enhanced anti-fibrotic effects against liver fibrosis," *International Journal of Molecular Sciences*, vol. 23, no. 10, p. 5420, 2022.

[27] Y. Wang, S. Zhang, Y. Zhang, J. Liu, F. Yang, and M. Xu, "Silymarin in cancer therapy: Mechanisms of action, protective roles in chemotherapy-induced toxicity, and nanoformulations," *Journal of Functional Foods*, vol. 100, p. 105384, Jan 2023.

[28] R. Ranasinghe, M. L. Mathai, and A. Zulli, "Cisplatin for cancer therapy and overcoming chemoresistance," *Heliyon*, vol. 8, no. 9, p. e10464, 2022.

[29] C. Schultheiss *et al.*, "The il-1β, il-6, and tnf cytokine triad is associated with post-acute sequelae of covid-19," *Cell Reports Medicine*, vol. 3, no. 6, p. 100663, 2022.

[30] H. Bahari *et al.*, "The effects of silymarin consumption on inflammation and oxidative stress in adults: a systematic review and meta-analysis," *Inflammopharmacology*, vol. 32, no. 2, pp. 949–963, 2024.

[31] F. Altındağ *et al.*, "Silymarin ameliorates cisplatin-induced nephrotoxicity by down-regulating tnf- and nf-kb and by upregulating il-10," *Journal of Experimental and Clinical Medicine*, vol. 39, no. 1, pp. 216–220, Jan 2022.

[32] A. Ramadhani, M. Hafiz, A. A. Putra, M. P. A. Nugroho, M. T. E. Awwal, I. Y. Prastyo, M. A. Muhtadi, S. Y. Azzahara, H. Mihardja, and S. N. Kurniawan, "Methylcobalamin as a candidate for chronic peripheral neuropathic pain therapy: Review of molecular pharmacology action," *The Korean Journal of Pain*, vol. 37, no. 4, pp. 299–309, Oct 2024.

[33] S. Vyloppilli *et al.*, "Safety and efficacy of methylcobalamin in the treatment of peripheral nerve injuries and diabetic neuropathies-a systematic review," *Acta Scientific Pharmaceutical Sciences*, vol. 5, no. 8, Aug 2021.

[34] K. Lis, "Desensitization for vitamin b12 hypersensitivity and how to do it," *Biomedicines*, vol. 13, no. 4, p. 801, Apr 2025.

[35] K. Halczuk, J. Kaziród, Z. Szic, J. Białecki, and K. Kasprzycka, "Vitamin b12—multifaceted in vivo functions and in vitro applications," *Nutrients*, vol. 15, no. 12, p. 2734, Jun 2023.

[36] J. A. Kellum *et al.*, "Acute kidney injury," *Nature Reviews Disease Primers*, vol. 7, no. 1, p. 52, 2021.

[37] A. M. Pisoschi *et al.*, "Oxidative stress mitigation by antioxidants—an overview on their chemistry and influences on health status," *European Journal of Medicinal Chemistry*, vol. 209, p. 112891, 2021.

[38] C. F. F. Festuccia, "Onconephrology: a new challenge for the nephrologist," in *Nephrology and Public Health Worldwide*, B. Geraldo, Ed. Cham: Springer, 2021, p. 91.

[39] R. Passos *et al.*, "Onconephrology: evolving concepts and challenges," *Frontiers in Nephrology*, p. 1585605, 2025.

[40] C. Tang, M. Darshi, K. Sharma, and Z. Dong, "Cisplatin nephrotoxicity: New insights and therapeutic implications," *Nature Reviews Nephrology*, vol. 19, no. 1, pp. 53–72, Jan 2023.

[41] N. V. Pervushin *et al.*, "Cisplatin resistance and metabolism: Simplification of complexity," *Cancers*, vol. 16, no. 17, p. 3082, 2024.

[42] R. M. d. C. Lyrio, M. M. S. Ferreira, and A. C. S. e. Silva, "Chemotherapy-induced acute kidney injury: Epidemiology, pathophysiology, and therapeutic approaches," *Frontiers in Nephrology*, vol. 4, p. 1436896, 2024.

[43] S. Mohammadi *et al.*, "Effects of silymarin supplementation on liver and kidney functions: A systematic review and dose–response meta-analysis," *Phytotherapy Research*, vol. 38, no. 5, pp. 2572–2593, 2024.

[44] Y. V. Shatalin *et al.*, "The redox-catalytic properties of cobalamins," *Molecular Biology*, vol. 57, no. 6, pp. 1038–1051, 2023.

[45] L. Díaz, R. Mondragón, R. García-Becerra, M. J. Ibarra-Sánchez, J. García-Quiroz, N. Santos-Martínez, E. Avila, and F. Larrea, "Ethical considerations in animal research: The principle of 3r's," *Revista de Investigación Clínica*, vol. 73, no. 4, pp. 199–209, Jul 2021.

[46] K. L. Navarro, M. T. Martin, H. E. Farag, J. A. Strickland, and A. J. Lowit, "Mouse anesthesia: The art and science," *ILAR Journal*, vol. 62, no. 1–2, pp. 238–273, 2021.

[47] D. L. Hickman, "Minimal exposure times for irreversible euthanasia with carbon dioxide in mice and rats," *Journal of the American Association for Laboratory Animal Science*, vol. 61, no. 3, pp. 283–286, May 2022.

[48] A. P. A. Kress, A. E. Cassano, and E. A. Nunamaker, "A comparison of blood collection techniques in mice and their effects on welfare," *Journal of the American Association for Laboratory Animal Science*, vol. 61, no. 3, pp. 287–295, May 2022.

[49] L. Charlès *et al.*, "Modified tail vein and penile vein puncture for blood sampling in the rat model," *Journal of Visualized Experiments (JoVE)*, no. 196, p. 65513, 2023.

[50] L. J. Yan, "Folic acid-induced animal model of kidney disease," *Animal Models and Experimental Medicine*, vol. 4, no. 4, pp. 329–342, Dec 2021.

[51] O. W. Griffith, "Determination of glutathione and glutathione disulfide using glutathione reductase and 2-vinylpyridine," *Analytical Biochemistry*, vol. 106, no. 1, pp. 207–212, Jul 1980.

[52] Y. Ye, Y. Wei, W. Liao, S. Li, X. Gu, J. Liu, W. Cai, and C. Ni, "Investigations into ferroptosis in methylmercury-induced acute kidney injury in mice," *Environmental Toxicology*, vol. 38, no. 6, pp. 1372–1383, Jun 2023.

[53] M. Zaguri, S. Aharon, and D. Hawlena, "Protein quantification in ecological studies: A literature review and empirical comparisons of standard methodologies," *Methods in Ecology and Evolution*, vol. 12, no. 7, pp. 1240–1251, Jul 2021.

[54] E. Rogatsky, "Pandora box of bca assay. investigation of the accuracy and linearity of the microplate bicinchoninic protein assay: Analytical challenges and method modifications to minimize systematic errors," *Analytical Biochemistry*, vol. 631, p. 114321, Oct 2021.

[55] M. Pohanka, O. Keresteš, and J. Žáková, "A 3d-printed do-it-yourself elisa plate reader as a biosensor tested on tnfα assay," *Biosensors*, vol. 14, no. 7, p. 331, 2024.

[56] A. A. Sattar *et al.*, "Rapid and effective protocol to measure glutathione peroxidase activity," *Bulletin of the National Research Centre*, vol. 48, no. 1, p. 100, 2024.

[57] R. C. Krieg *et al.*, "Protein quantification and its tolerance for different interfering reagents using the bca-method with regard to 2d sds page," *Journal of Biochemical and Biophysical Methods*, vol. 65, no. 1, pp. 13–19, 2005.

[58] M. Kumar *et al.*, "Predictive biomarkers for anti-tnfα therapy in ibd patients," *Journal of Translational Medicine*, vol. 22, no. 1, p. 284, 2024.

[59] F. Pan *et al.*, "Nadphnet: a novel strategy to predict compounds for regulation of nadph metabolism via network-based methods," *Acta Pharmacologica Sinica*, vol. 45, no. 10, pp. 2199–2211, 2024.